Regulation of Lysosomal Function by the DAF-16 Forkhead Transcription Factor Couples Reproduction to Aging in *Caenorhabditis elegans*

Kunal Baxi,*[,1,2] Ata Ghavidel,[†,1] Brandon Waddell,* Troy A. Harkness,[†] and Carlos E. de Carvalho*[,3]
*Department of Biology and [†]Department of Anatomy and Cell Biology, University of Saskatchewan, Saskatoon, Saskatchewan S7N5E2, Canada

ABSTRACT Aging in eukaryotes is accompanied by widespread deterioration of the somatic tissue. Yet, abolishing germ cells delays the age-dependent somatic decline in *Caenorhabditis elegans*. In adult worms lacking germ cells, the activation of the DAF-9/DAF-12 steroid signaling pathway in the gonad recruits DAF-16 activity in the intestine to promote longevity-associated phenotypes. However, the impact of this pathway on the fitness of normally reproducing animals is less clear. Here, we explore the link between progeny production and somatic aging and identify the loss of lysosomal acidity—a critical regulator of the proteolytic output of these organelles—as a novel biomarker of aging in *C. elegans*. The increase in lysosomal pH in older worms is not a passive consequence of aging, but instead is timed with the cessation of reproduction, and correlates with the reduction in proteostasis in early adult life. Our results further implicate the steroid signaling pathway and DAF-16 in dynamically regulating lysosomal pH in the intestine of wild-type worms in response to the reproductive cycle. In the intestine of reproducing worms, DAF-16 promotes acidic lysosomes by upregulating the expression of v-ATPase genes. These findings support a model in which protein clearance in the soma is linked to reproduction in the gonad via the active regulation of lysosomal acidification.

KEYWORDS DAF-16; acidity; lysosome; reproduction; v-ATPase; *C. elegans*

THE germline has an active role in regulating lifespan across eukaryotes. In *C. elegans*, removing germ cells delays age-dependent somatic deterioration and significantly increases lifespan (Hsin and Kenyon 1999; Antebi *et al.* 2000; Berman and Kenyon 2006; Ghazi *et al.* 2009). The longevity in germ cell-depleted animals is regulated by signals from the gonad, and is not a simple consequence of sterility, since ablation of the somatic gonad in addition to germ cells suppresses this effect (Hsin and Kenyon 1999). Eliminating germ cells during adulthood in *Drosophila* (Flatt *et al.* 2008) or transplanting ovaries of young mice into older animals similarly promotes lifespan extension (Cargill *et al.* 2003), underscoring the evolutionary conservation of gonad to soma communication in regulating fitness.

Several studies have pointed to different signaling pathways implicated in the gonad-dependent regulation of aging in *C. elegans*. These pathways link germ cell proliferation in the distal gonad to the transcriptional activities in somatic cells of the nuclear receptors DAF-12 and NHR-80 as well as the Forkhead proteins PHA-4 and DAF-16. Together, these effectors establish complex transcriptional networks functionally linking soma and germline through the regulation of protein synthesis rates, protein folding, autophagy, metabolic adaptation, pathogen resistance, lipid metabolism, and response to stress (reviewed in Antebi 2013). Converging downstream in these signaling networks is the activity of the Forkhead transcription factor DAF-16 in the intestine—the major metabolic and endocrine organ in *C. elegans*. Mechanistically, DAF-16 activation relies on post-transcriptional modifications that control its access to the nucleus. As a target of insulin/IGF (IIS) signaling, DAF-16 is phosphorylated by activated AKT, resulting in its nuclear exclusion and transcriptional inhibition (Kenyon 2010b). In mutants with

doi: https://doi.org/10.1534/genetics.117.204222
Manuscript received May 30, 2017; accepted for publication July 3, 2017; published Early Online July 7, 2017.
Supplemental material is available online at www.genetics.org/lookup/suppl/doi:10.1534/genetics.117.204222/-/DC1.
[1]These authors contributed equally to this work.
[2]Present address: Greehey Children's Cancer Research Institute, UT Health Sciences Center, San Antonio, TX 78229
[3]Corresponding author: Department of Biology, University of Saskatchewan, 112 Science Place, Saskatoon, SK S7N5E2, Canada. E-mail: carlos.carvalho@usask.ca

impaired or reduced insulin/IGF signaling, dephosphorylated DAF-16/FOXO constitutively localizes to the nucleus, where it promotes lifespan extension from yeast to mammals (Kenyon 2005; DiLoreto and Murphy 2015). DAF-16 nuclear localization in germ cell proliferation mutants, however, appears to be regulated independently of IIS inputs (Berman and Kenyon 2006). Instead, factors such as the 14-3-3 protein FTT-2 and KRIT/KRI-1 specifically influence intestinal DAF-16 nuclear presence in response to signals from the gonad (Berman and Kenyon 2006; Li *et al.* 2007). Moreover, genes involved in steroidogenesis such as *daf-9*, *daf-36*/Rieske oxygenase, and the β-hydroxysteroid dehydrogenase *dhs-16*, act through DAF-12 to impact DAF-16 function in the intestine, pointing to a critical role of steroidal signaling in mediating the cross-talk between soma and germ cells (Rottiers *et al.* 2006; Gerisch *et al.* 2007; Shen *et al.* 2012). Finally, neuronal expression of a microRNA (*mir-71*) has been linked to DAF-16 nuclear accumulation in intestinal cells, likely in a gonad-dependent manner (Boulias and Horvitz 2012). These important studies using sterile mutants exposed functional ties between reproduction and aging, and underscored the complexity in regulating DAF-16 activity in the intestine. However, whether intestinal DAF-16 is sensitive to the critical transition between reproductive and postreproductive periods, when several aging-related phenotypes first appear, has not been rigorously examined (Herndon *et al.* 2002; McGee *et al.* 2011; Liu *et al.* 2013).

A prominent aging-related phenotype is the appearance of detergent insoluble protein inclusions in old eukaryotic cells (Rubinsztein 2006; Erjavec *et al.* 2007; Madeo *et al.* 2009). The accumulation of misfolded and irreversibly modified proteins into large aggregates accompanies, and is thought to be among, the primary causes of cellular senescence (Muchowski 2002; Cuervo *et al.* 2005; Cohen *et al.* 2006; Harrington *et al.* 2011). In *C. elegans*, a sudden decline in proteostasis, and the subsequent accumulation of protein aggregates is observed in the soma during early adulthood and depends on germ cell proliferation (Ben-Zvi *et al.* 2009; Shai *et al.* 2014; Labbadia and Morimoto 2015). In turn, germ-cell-deprived mutants show increased proteasome activity in the soma via DAF-16-dependent upregulation of RPN-6.1—a subunit of the 19S proteasome (Vilchez *et al.* 2012). These studies point to the nonautonomous regulation of protective mechanisms against proteotoxicity by the gonad during the transition to reproductive maturity. It is less clear, however, whether the appearance of cellular signatures of proteotoxic stress is subsequently influenced by the reproductive cycle, and what is the role of lysosomal-mediated proteolysis in this process.

Here, we hypothesize that protein clearance via the lysosomal degradation pathway in the soma may be sensitive to reproductive signals from the gonad. Lysosomes constitute the end point of different degradation pathways in the cell, and are important mediators in several signaling events. These recycling organelles are involved in processes as diverse as autophagy, membrane repair, transcriptional control, and nutrient sensing, highlighting their centralizing role in the context of cellular and tissue homeostasis (reviewed in Lim and Zoncu 2016). Age-dependent decreases in lysosomal function have been linked to several progressive degenerative disorders that strike later in life (reviewed in Boya 2012). Restoring function to lysosomes can slow down the late onset phenotypes associated with these conditions, suggesting that lysosomes may be relevant targets for antiaging manipulations in humans (Vila *et al.* 2011; Kim *et al.* 2016). The close relationship between lysosomes and aging underscores the importance of elucidating the molecular mechanisms leading to loss of lysosomal function in senescing cells. The network of lysosomal proteases maintains comparable expression in aging cells such that changes in enzyme load is unlikely to be the primary cause for the collapse in lysosomal-mediated degradation observed in old cells (Cuervo and Dice 2000; Brunk and Terman 2002a; Lund *et al.* 2002; Golden and Melov 2004). Loss of vacuolar acidity, on the other hand, has been recently proposed to decrease yeast replicative lifespan in part by triggering age-dependent mitochondrial dysfunction (Hughes and Gottschling 2012). It is possible, therefore, that aging is antagonized by mechanisms that actively maintain a low lysosomal pH in multicellular organisms, a process that ultimately relies on the activity of v-ATPases—a family of conserved proton pumps assembled on the lysosomal membrane. Here, we present evidence of one such mechanism in *C. elegans*, and demonstrate that it is regulated by signals from the progeny-producing gonad to affect somatic tissues, suggesting that one of its possible roles may be to synchronize reproduction and aging. Our results indicate that lysosomal pH in *C. elegans* is regulated by changes in the reproductive cycle via the transcriptional control of v-ATPases. Through our investigations of the genetic network coordinating these events, we implicate the DAF-9/DAF-12/DAF-16 signaling axis, previously shown to regulate longevity in germ cell-depleted mutants, and introduce lysosomal pH as a novel cellular readout for gonad to soma communication. These results expose a conserved eukaryotic mechanism linking proliferation/reproduction to cellular homeostasis and aging through the control of lysosomal function.

Materials and Methods

C. elegans strains and husbandry

Worms were maintained on NGM plates at standard growth conditions (20°) unless indicated otherwise. To generate sterile animals, temperature-sensitive mutants were synchronized by bleaching, L1 diapause larvae were collected 15 hr later and transferred to NGM-OP50 plates. Larvae were allowed to develop at 25° for a further 24 hr before being transferred back to 20° for the rest of the experiment. Mating experiments were performed by adding five males to one female (*fem-2*) or hermaphrodite (N2) ratio on plates with a small bacterial lawn. Worms were removed after 4 hr to fresh OP50 plates. A list of strains used in this study and RNAi protocols are available in Supplemental Material, File S1.

cDCFDA staining

In every experiment, NGM plates from the same batch with a standardized ~2 × 2 cm OP50 lawn were used; 100 μl of 10 mM cDCFDA (Molecular Probes) was pipetted to cover the entire lawn and left to dry in the dark for 10 min. Around 15–20 worms from synchronized populations were placed on the OP50/cDCFDA lawn and incubated for 14–16 hr at 20° protected from light. Prior to imaging, worms were moved to NGM plates without bacteria for 15 min to clear from excess dye. Shortly before imaging, 2% agarose pads of similar thickness were prepared using the same agarose solution. Worms were anesthetized in 5 mM sodium azide, and immediately imaged using a Zeiss LSM 510 confocal microscope. Prior to imaging, to normalize variations in fluorescent signals among different experiments, 2-day-old N2 worms that consistently showed strong cDCFDA signal were used to calibrate capture parameters such as pinhole and aperture such that the average fluorescent intensity (see below for signal quantification) was ~400 AU at 520 nm. This established a signal threshold against which the other samples in the same experiment could be compared, and allowed a broad range of signal intensities to be imaged without any further postacquisition manipulation. These conditions were reset prior to every imaging session to ensure consistency in image acquisition in different staining experiments, accounting for potential differences in dye intake. After adjusting the focus, single plane images were taken using a 60× lens and a resolution of 1024 × 1024 pixels. The cDCFDA emission spectra in worms yielded a single prominent peak at 520 nm coinciding with its reported fluorescence spectra (Preston *et al.* 1989), providing a specific signal readout distinct from intestinal autofluorescence. In order to quantify cDCFDA fluorescence intensity, the Zeiss LSM image acquisition software was used. Briefly, four to five regions of interest (ROI) corresponding to four to five different in-focus lysosomes per image were selected, and the average relative fluorescence intensity of each ROI was calculated for an emission spectra ranging from 500 to 550 nm. This was done for at least four to five lysosomes per worm for about four to six worms per genotype, resulting in a total of ~25–30 different lysosomal fluorescence intensities for each genotype. No signal postacquisition signal enhancement was performed. Blind tests with N2 and *fem-2* worms were often done to assess potential experimental bias.

Costaining with other lysosomal marker dyes

Fluorescent dyes in M9 buffer were added to OP50 lawns at the following concentrations: Nile Red (Sigma-Aldrich): 50 μl of a 15 μg/ml, LTR DND-99 (Molecular Probes) 2.5 μl of a 1 mM solution, and LSG-DND-189 (Molecular Probes) 2.5 μl of a 1 mM solution. After drying, 15–20 worms were added on OP50/dye plates and incubated protected from light. Incubation times at 20° were overnight for cDCFDA and Nile Red staining, and 5 min for LSG and LTR. Imaging of live worms was performed immediately after mounting animals on slides as described for cDCFDA staining. To allow for direct and reliable comparison in costaining experiments, young and old worms were stained at the same time using the same staining solution and imaging acquisition parameters. After normalizing for background fluorescence, signal intensity values for both dyes were collected individually for each selected lysosome as described above. At least five lysosomes per image were randomly selected for quantification. Fluorescence intensity values for each lysosome were then used to calculate the green over red (LSG or cDCFDA/LTR) ratios. The ratio averages for each image were then generated to plot the graphs in Figure 1, D and F. Intestines from over 15 worms in each treatment were used in the quantification.

Chloroquine treatment

For incubations with chloroquine (Sigma), worms were synchronized by bleaching and grown until L4 on NGM/OP50 plates. Thereafter, they were transferred onto plates supplemented with 200 mM chloroquine, and grown until day 2 post L4. Then, 10 mM cDCFDA was added to the plates, and the worms imaged 24 hr later using a Zeiss LSM 510 confocal microscope.

Immunostaining of intestinal cells and imaging

Worms were dissected on glass cover slips in M9 Buffer, and then freeze-cracked on an aluminum block on dry ice. Dissected intestines were fixed, blocked and incubated with primary antibodies overnight. Protocol details can be found in File S1.

Δ^4-Dafachronic acid (DA) feeding protocol

Synchronized worms were incubated from L4 stage onwards on (a) NGM plates with OP50 supplemented with freshly made 1, 10, or 100 μM DA, or (b) NGM plates with OP50 supplemented with ethanol (control). For cDCFDA analysis following DA feeding, worms were transferred every day to fresh NGM plates supplemented with ethanol with DA; 100 μM cDCFDA was added to NGM plates containing OP50 (with or without DA). Worms were grown overnight on these plates for at least 14–16 hr and then used for microscopy.

Generation of the SEP::mCherry::LAAT-1 line

A synthesized 2.1 kb SEP::mCherry::*laat-1* cDNA cassette was directionally cloned between the muscle-specific *unc-54* 5′ and 3′ regulatory sequences of pPD30.38 using *Kpn*I/*Sac*I sites (Mello and Fire 1995). In this construct, SEP and mCherry sequences are separated by a 21-bp linker sequence (5′-GGTGGAGGAGGTAGATCCATG-3′), and an HA tag is also added to the C (cytosolic) terminus (Tanida *et al.* 2014). Stable transgenic lines were generated in an N2 (wild-type) background by gonad microinjection using a dominant allele of *rol-6* as a coinjecting marker. We followed the age synchronization, live imaging and chloroquine treatment protocols described above and in File S1 to assess muscle SEP and mCherry signals in young and old worms.

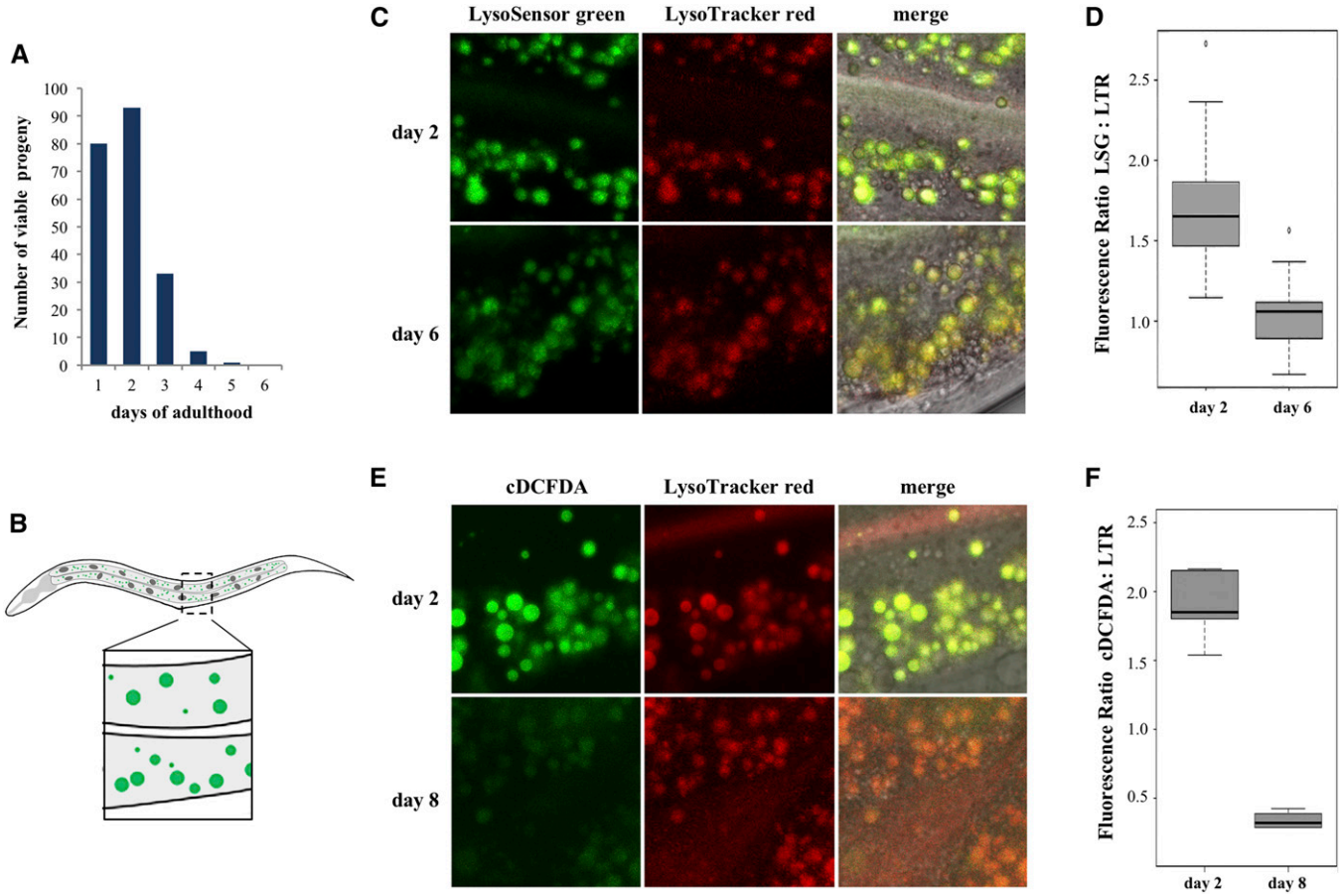

Figure 1 *In vivo* assessment of lysosomal acidity in *C. elegans* intestines. (A) Representative reproduction timeline of wild-type hermaphrodites grown at 20°. (B) Diagram of a worm illustrating the midbody region in the intestine considered for subsequent image analysis of lysosomes (green spots in inset). (C) Representative images of intestines of day 2 (reproductive) and day 6 (postreproductive) worms costained with LSG DND-189 and LTR DND-99. (D) LSG/LTR average ratios for day 2 and day 6 animals. (E) Representative images of intestines of day 2 and day 6 worms costained with cDCFDA and LTR DND-99. (F) cDCFDA/LTR average ratios for day 2 and day 6 animals.

RT and qPCR analyses

RNA was extracted from 10 adult animals using Trizol (Invitrogen). After a 30 min DNase I (Fermentas) treatment, cDNA was synthesized using iScript cDNA Synthesis Kit (Bio-Rad); 10 ng of cDNA was used in real-time PCR amplification using the iQ SYBR Green Supermix (Bio-Rad) and the iCycler system (Bio-Rad). The relative expression level of each gene was determined using the Comparative CT Method, and normalized to 28S rRNA internal control in the same sample. Measurements were performed in triplicate for two biological samples for each condition. Single worm RT-PCR was performed using the One-Step RT-PCR system (Invitrogen) according to the manufacturer's instructions. A list of primers used is available in Table S2.

Western blot analysis

Lysates from ~300 worms were prepared in denaturing conditions. A rabbit polyclonal DAF-16 antibody (#33738; Santa Cruz) was used at 1/2000. β-Actin and GFP antibodies (Abcam) were used at 1/5000. The chemiluminescent blots were imaged with a ChemiDoc MP imager (Bio-Rad). Image-Lab software version 4.1 (Bio-Rad) was used for image acquisition and densitometric analysis. Protocol details can be found in File S1.

Worm tracking

Three age-matched worms in each treatment were randomly picked and placed on a fresh NGM plate. Movies were recorded for 30 sec to 1 min using a Basler acA2500 camera mounted on a Nikon 60 mm f/2.8D micro lens. Videos were subsequently processed using WormLab v4.05 (MBF Bioscience).

Data availability

Strains are available upon request. File S1 contains detailed descriptions of all Supplemental Materials and Methods. File S2 and File S3 are videos showing motility of 8-day-old N2 and *fem-2* worms, respectively. Table S1 contains lifespan data for different mutants. Table S2 contains primers used in this study.

Results

Rise in lysosomal pH in the intestine of postreproductive C. elegans

In adult *C. elegans*, after an initial period of egg laying, reproduction in self-fertile hermaphrodites sharply decreases on day 3 of adult life (day 1 standardized as 24 hr post-L4 molt at 20°), then ceases at around days 5–6 due to the depletion of the sperm repository (Kimble and Crittenden 2005) (Figure 1A). In yeast, reduced vacuolar acidification in aging cells signals the end of replicative lifespan (Hughes and Gottschling 2012). To address whether loss of acidity in lysosomes is a conserved event marking the end of reproductive life in in *C. elegans*, we first examined whether the transition between reproductive and nonreproductive periods correlated with changes in lysosomal pH in the intestine—a tissue known to respond to signals from the gonad (Mukhopadhyay and Tissenbaum 2007). Worms were fed the fluorescent pH-indicators LysoSensor Green DND-189 (LSG, pKa 5.2), or 5-(and-6)-Carboxy-2′,7′-Dichlorofluorescein Diacetate (cDCFDA, pKa 4.8); both probes are commonly used to track lysosomal pH in live cells (Nedergaard *et al.* 1990; Horn *et al.* 1992; Kosegarten *et al.* 1997; Harrison *et al.* 2002; Levitte *et al.* 2010; Farkas *et al.* 2015; Ho *et al.* 2015). LSG is a small acidotropic probe, while cDCFDA is a ROS-insensitive derivative of DCFDA (Peri and Nusslein-Volhard 2008; Vibet *et al.* 2008). Protonation of LSG molecules and hydrolysis of cDCFDA into the impermeable fluorescent moiety 6-carboxyfluorescein trap these dyes inside acidic vesicles, wherein their fluorescence increases with decreasing pH (Preston *et al.* 1989). To control for variations in dye intake, intestines were costained with LysoTracker Red DND-99 (LTR), a weak amine based-dye that marks acidic compartments over a broad pH range, and whose fluorescence is largely insensitive to increasing acidity (Duvvuri *et al.* 2004). When included as food supplements, LSG, cDCFDA, and LTR passively crossed the apical membrane of intestinal cells where they were observed to fully colocalize within cytoplasmic vesicles (Figure 1, B, C, and E). For simplicity, we refer to these acidic vesicles as lysosomes, though they could also include other lysosome-related organelles such as acidifying endosomes (Clokey and Jacobson 1986; Hermann *et al.* 2005). We noticed a significant reduction ($P < 0.001$ by the Student *t*-test) in the green/red (LSG or cDCFDA/LTR) fluorescence intensity ratios in the intestine of postreproductive worms (day 6 or 8) as compared with reproducing animals (day 2) (Figure 1, C and E, quantified in Figure 1, D and F). The decreased ratio observed with cDCFDA, compared with LSG (compare Figure 1D with Figure 1F), likely reflects different pKa values for these dyes, with cDCFDA fluorescence being more sensitive to incremental changes in pH. We therefore used cDCFDA in controlled staining experiments (see *Materials and Methods*) as an *in situ* probe to capture a timeline of lysosomal acidity in aging wild-type animals. As depicted in Figure 2A, actively reproducing worms displayed high cDCFDA fluorescence (day 1–3). In contrast, loss of acidity, indicated by a marked reduction in cDCFDA fluorescence ($P < 0.001$ by the Student *t*-test), occurred abruptly between day 3 and day 6 of adulthood, and did not recover afterward (quantified in Figure 2A, lower panel). Temporally, the pH increase in intestinal lysosomes parallels the sharp drop in reproductive outputs during the same period (Figure 1A). Lysosomal pH is maintained by an evolutionarily conserved, multi-subunit proton-coupled ATPase pump (v-ATPase) (Preston *et al.* 1992; Lee *et al.* 2010). In *C. elegans*, at least 21 v-ATPase (*vha*) genes encode subunits make up the peripheral (V_1) domain involved in ATP hydrolysis and the transmembrane rotor (V_0) domain that translocates protons from the cytosol to the lumen (Lee *et al.* 2010) (Figure 2B). Importantly, cDCFDA fluorescence was sensitive to RNAi knockdown of a V_1 (*vha-8*) or a V_0 (*vha-2*; $P < 0.0001$ by the Student *t*-test) subunits of the proton pump, or treatment with the lysosomotropic agent chloroquine ($P < 0.0001$ by the Student *t*-test), which inhibits acidification (Figure 2C, quantified in lower panel).

The results above predict that lysosome-dependent degradation of protein aggregates may be impaired following the transition from reproductive to postreproductive life. In particular, the breakdown of large protein inclusions not amenable to refolding by molecular chaperones or degradation by proteasomes could be affected (Cuervo *et al.* 2005; Mohri-Shiomi and Garsin 2008). Taking advantage of a polyglutamine (polyQ) aggregate model in *C. elegans* that has been used to assess the proteolytic capacity of cells *in vivo* (Burkewitz *et al.* 2012), we asked whether aggregation of a Q64::YFP fusion protein ectopically expressed in the intestine was coincident with the end of reproduction. We observed that in intestinal cells of reproducing (day 2) worms, lysosomes, marked by Nile Red staining (O'Rourke *et al.* 2009; Soukas *et al.* 2013), were largely devoid of YFP fluorescence. In contrast, polyQ aggregates accumulated in the lysosomal lumen of postreproductive (day 6) worms (Figure S1A). Proteolysis of Q64::YFP in young worms released a stable YFP moiety (Holmberg *et al.* 2004), detected as a discrete fragment by SDS-PAGE. As opposed to young worms, cleavage of the YFP moiety in postreproductive (day 6 and older) worms was reduced (Figure S1B). These results are consistent with a rise in pH in intestinal lysosomes of postreproductive worms leading to impaired clearance of protein aggregates.

Sterility delays lysosomal alkalinization in the intestine

One interpretation of our findings is that the transition from reproduction to postreproduction signals lysosomal alkalinization in the intestine leading to reduced proteolysis in the soma, and ultimately senescence. Progeny production in hermaphrodites is normally limited by sperm repository, as well as a decline in oocyte quality, which, over time, contribute to reproductive cessation (Hughes *et al.* 2007; Luo *et al.* 2010). In this context, reduced fertilization due to sperm depletion or progressive loss of oocyte fertilizability could plausibly trigger gonadal signaling to the soma. If so, disruption of signaling from the gonad in sterile mutants should result in prolonged maintenance of

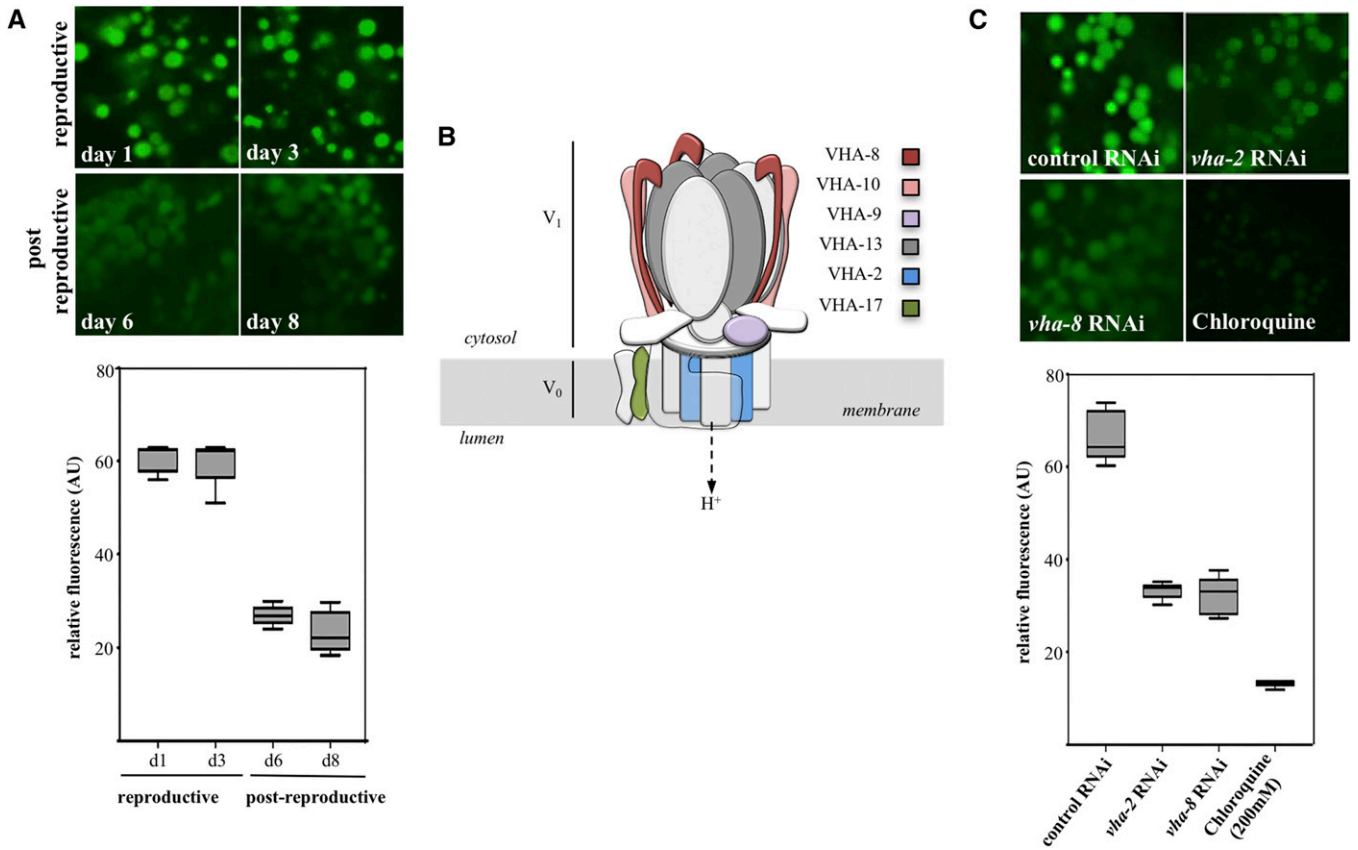

Figure 2 Loss of lysosome acidity in the transition to postreproductive life. (A) cDCFDA imaging of intestinal lysosomes in wild-type reproductive (day 1 and 3) and postreproductive (day 6 and 8) stages. The corresponding quantified average fluorescent values are shown in the bottom. The differences in signal intensities between day 1 and 3 (reproductive) and day 6 and 8 (postreproductive) were not significant (P = 0.8203 and P = 0.1496, respectively). (B) Schematic representation of the v-ATPase complex assembled on the lysosomal membrane. The subunits mentioned in this work are indicated. (C) cDCFDA imaging of intestinal lysosomes of worms in reproductive stage (day 2) after control RNAi, *vha-2* RNAi, *vha-8* RNA or treatment with 200 mM of chloroquine. The corresponding quantified average fluorescent values are shown in the bottom. The difference between cDCFDA signals between the RNAi knockdowns of the two protein pumps was not significant (P = 0.5922).

lysosome acidity in the intestine. To test this idea, we examined the dynamics of pH changes in intestinal lysosomes of three sterile mutants that either do not produce mature germ cells (sperm and oocytes), or make viable oocytes but not sperm (self-sterile). Eliminating GLP-1 activity [using a *glp-1*(*e2141*) mutant] abolishes germ cell proliferation (Hutter and Schnabel 1994), resulting in an "empty gonad" phenotype and extended lifespan (Arantes-Oliveira *et al.* 2002). *fem-2*(*b245ts*) and *spe-26*(*hc140ts*) worms grown at restrictive conditions produce fertilizable oocytes, but no (*fem-2*) or very few (*spe-26*) self-fertilized progeny due to feminization of the germline (*fem-2*) or impaired spermatogenesis (*spe-26*) (Pilgrim *et al.* 1995; Varkey *et al.* 1995). We found that, unlike wild-type hermaphrodites, *glp-1*, *fem-2*, and *spe-26* sterile worms maintained acidic lysosomes past day 6 of adulthood (Figure 3A, quantified in Figure 3B). Moreover, similar to *glp-1* (Arantes-Oliveira *et al.* 2002) and *spe-26* (Gems and Riddle 1996), lifespan of *fem-2* mutants was also extended, suggesting that prolonged lysosome acidity may be one contributing factor to the longevity phenotype in these mutants (Figure 3C). The metabolic requirement for oogenesis is among the most resource intensive developmental undertakings in adult hermaphrodites (Rose and Kemphues 1998). *fem-2* and *spe-26* worms, producing a full complement of oocytes, nevertheless displayed a profile of cDCFDA staining in postreproductive age indistinguishable from *glp-1* worms (at day 8, P = 0.0560 and P = 0.4406 by the Welch two sample t-test, respectively). The maintenance of lysosomal acidity in sterile worms therefore cannot be fully explained by resource reallocation from gamete producing gonads to the soma (Kirkwood 1977), and may instead involve an impairment in signaling the functional decline of lysosomes in animals that fail to reproduce.

To further investigate the apparent link between fertilization in the gonad and lysosome acidity in the soma, we mated female *fem-2* worms with wild-type males to restore progeny production. Mating has been shown to reduce the average lifespan of feminized worms independent of receipt or storage of sperm, brood size, or structural damage during copulation (Gems and Riddle 1996; Shi and Murphy 2014). We found that reinstating progeny production in *fem-2* worms suppressed its long-lived phenotype (Figure 3C), and was sufficient to accelerate the loss of lysosome acidity with a cDCFDA staining profile similar (P = 0.0967 by the Welch two sample t-test) to the age-matched day 8 wild-type

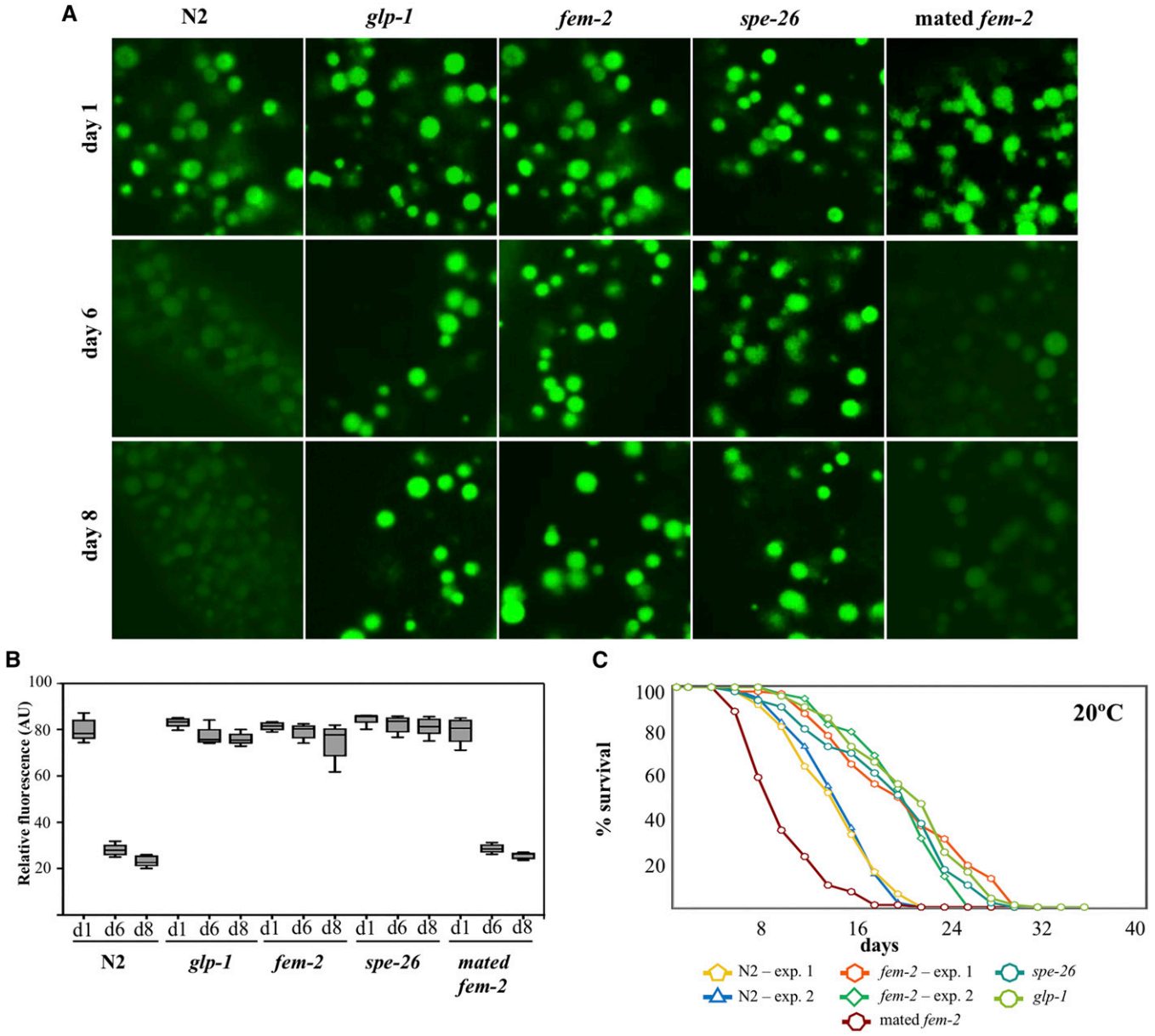

Figure 3 Delayed loss of lysosomal acidity in sterile worms. (A) cDCFDA staining of intestinal lysosomes in age-matched wild-type, *fem-2*, *spe-26* (sperm-less mutants) and *glp-1* (germ-cell-less) and mated (reproducing) *fem-2* mutants. (B) Quantification of cDCFDA signal intensity in age-matched sterile mutants in day 1 (d1), day 6 (d6), and day 8 (d8) of adulthood. Animals that fail to produce germ cells (*glp-1* mutants) or to fertilize (*fem-2*, *spe-26* mutants) have a similar cDCFDA signal intensity compared to wild-type worms during the reproductive period (day 1: *glp-1* $P = 0.1876$; *fem-2* $P = 0.4759$, and *spe-26* $P = 0.0744$), but show significantly higher cDCFDA signals past the reproductive age ($P < 0.0001$). (C) Lifespan analysis of wild-type animals relative to sterile *fem-2*, *spe-26*, *glp-1*, and mated (progeny producing) *fem-2* worms. ($P < 0.0001$, Mantel-Cox test).

worms (Figure 3A, quantified in Figure 3B). Taken together, these observations support a scenario in which lysosomal pH in the intestine of wild-type worms is temporally coupled to the reproductive state in the gonad.

Protein aggregation in muscle cells increases postreproduction

Widespread protein insolubility leading to formation of protein aggregates in several tissues underlies aging in *C. elegans* (David *et al.* 2010; Liang *et al.* 2014). We therefore sought evidence to show that the impairment in lysosomal function due to a rise in lysosomal pH in postreproductive worms was not limited to the intestine. Age-related muscle degeneration (sarcopenia) leading to muscle loss and defects in locomotion is particularly conspicuous in worms. The first signs of muscle tissue decline are detectable early in postreproductive life, at day 7 of adulthood (Herndon *et al.* 2002). Since cDCFDA does not cross the basal lamina of the intestine, we used instead a transgenic approach to investigate whether the lysosomal pH in muscle cells also changes in postreproductive

animals. We produced *in vivo* pH sensor strains expressing a fusion between the pH-sensitive GFP-derived superecliptic pHluorin (SEP) and the pH-insensitive mCherry in muscle cells (Hughes and Gottschling 2012; Tanida *et al.* 2014). The SEP::mCherry cassette was then fused to the N-terminus of the amino-acid transporter LAAT-1 on the lysosomal membrane, facing the acidic lumen (Liu *et al.* 2012). With a pKa of 7.6, SEP fluorescence is quenched when the pH is below 6.5, and only residual signal can be observed in normally acidic (pH 4.5) lysosomes (Sankaranarayanan *et al.* 2000; Tanida *et al.* 2014). Similar to the reported morphology of muscle lysosomes in *C. elegans* (Li *et al.* 2016), conspicuous mCherry fluorescence was observed in globular and tubular organelles equally present in cells of young and old animals. In contrast, day 2 (reproducing) animals showed only diffuse SEP fluorescence in the cytoplasm, likely representing SEP::mCherry::LAAT-1 at neutral cytosolic pH before association to mature lysosomes (Figure 4A, upper panels, quantified in Figure 4B). In day 10 post-L4, around the midpoint in the average lifespan of *C. elegans* and several days after the end of progeny generation, we noticed a small (16–24%), but reproducible, proportion of animals with muscle cells in which SEP and mCherry signals colocalized in lysosome-like structures (Figure 4A, middle panels, quantified in Figure 4B). The low frequency of SEP-positive cells in these experiments may be explained by the requirement of nearly complete deacidification of lysosomes before they can be captured by SEP fluorescence. Consistent with this, treatment with 200 mM chloroquine, which leads to a substantial loss in acidity in the intestine of day 2 worms (Figure 2C), resulted in only ~36% of animals with cells showing SEP signal in lysosomes (Figure 4A, lower panels, quantified in Figure 4B). We reasoned that SEP-positive organelles in muscle represented the fraction of alkalinizing lysosomes that had reached pH values above 6 by day 10. In physiological terms, however, a much less intense rise in pH can have dramatic consequences to lysosomal function (Ahlberg *et al.* 1985; Colacurcio and Nixon 2016). It is possible, therefore, that lysosomal alkalinization is more widespread in muscle cells of postreproductive *C. elegans* than was detected using the SEP::mCherry sensor.

If lysosomal dysfunction in muscle cells is indeed timed with the end of reproduction, this may signal the early signs of proteolytic impairment in muscle tissue of postreproductive animals. The role of lysosome-mediated proteolysis in the regulation of protein aggregation and clearance in muscle has been studied in *C. elegans* using transgenic lines expressing human α-synuclein (α-syn) (Qiao *et al.* 2008; Ghavidel *et al.* 2015; Kim *et al.* 2016). To determine whether loss of lysosomal acidity in muscle cells has functional consequences in turnover of protein aggregates, we examined the accumulation of α-syn::GFP aggregates resulting from an ectopically expressed, muscle-directed transgene ($P_{unc\text{-}54}$::α-syn::GFP; Harrington *et al.* 2011). Protein aggregation, as detected by GFP foci formation, was prominent in postreproductive (day 8) wild-type worms (Figure 4C). In contrast, age-matched feminized (grown at 25°), but not self-fertile (grown at 16°) day 6 *fem-2* animals displayed a significant reduction ($P < 0.001$ by the Welch two sample *t*-test) in the number of *in situ* GFP foci in the midbody region (Figure 4C, quantified in Figure 4D). Consistent with improved maintenance of acidic lysosomes in sterile mutants, the absence of α−syn::GFP aggregation in the muscle of *fem-2* females was accompanied by α−syn::GFP degradation (Figure S2A, quantified in Figure S2B). Finally, the enhanced clearance of protein aggregates in muscle of *fem-2* worms was also conserved in *glp-1* and *spe-26* sterile mutants (Figure S2C). Together, these results indicate that loss of acidity in *C. elegans* intestinal lysosomes extends to muscle tissue, where it likely contributes to a global decline in proteostasis in early adulthood.

DAF-16 upregulates v-ATPAse gene expression in reproducing worms

Next, we sought to elucidate the mechanistic basis for lysosomal alkalinization in postreproductive wild-type worms. Using qRT-PCR, we observed that the *vha-2* and the *vha-8* components of the v-ATPase complex displayed reduced transcript abundance during the latter days of reproduction (Figure 2B, Figure 5, A and B, and Figure S3). This reduction in transcript levels occurred by days 4–5 of adulthood, corresponding to the end of progeny production and preceding the loss of lysosome acidity. In contrast, feminized *fem-2* worms maintained high *vha* mRNA levels throughout the corresponding period. Similar increases in v-ATPase mRNA abundance have been previously described in *glp-1* mutants (Lapierre *et al.* 2013). Moreover, mating *fem-2* females was sufficient to reduce *vha* transcript abundance with a kinetics similar to that observed in wild-type hermaphrodites (Figure 5, A and B). To account for the contribution of nonintestinal v-ATPase gene transcription in the whole animal *in vitro* analysis described above, we produced a line expressing a transcriptional reporter for *vha-2* (*Pvha-2*::*GFP*) and individually assessed whether intestinal GFP signals in the same animal changed in the transition between reproductive and postreproductive periods (Figure S4, A and C). As previously reported (Oka *et al.* 1997), *vha-2* expression was observed in the H-shaped excretory cells and in the adult intestine (Figure S4A). While GFP signals in the excretory cell in the head region appeared equivalent in day 2 and day 6, in 81% of the worms followed ($n = 21$) *Pvha-2*::*GFP* expression in the most anterior intestinal cell (int1) was reduced by day 6 (Figure S4, A and C). In summary, these results suggest that the loss of lysosomal acidity in postreproductive worms follows the downregulation in *vha* gene transcription.

The coordinated decline in v-ATPase transcripts could in theory account for the lumen alkalinization observed in intestinal lysosomes. In *C. elegans*, the transcriptional activity of DAF-16 in the intestine is modulated by signals from the gonad (Hsin and Kenyon 1999; Hsu *et al.* 2003). Notably, the V_0 subunit *vha-3*, which is predominantly expressed in the intestine (Oka *et al.* 1998), was identified as a DAF-16 target gene in a Chromatin Immunoprecipitation (ChIP)

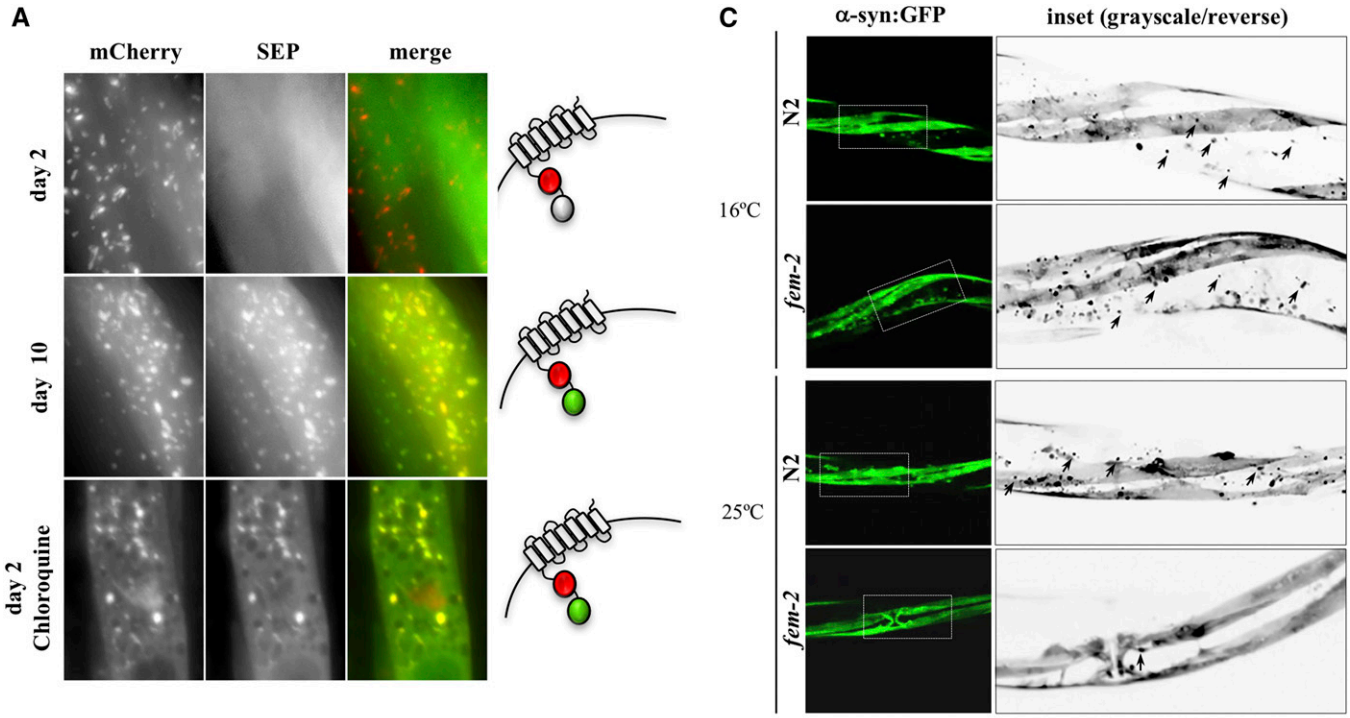

B

		with lysosomal SEP	(n)
day 2	line 1 *exp.1*	0 (0%)	50
	line 1 *exp.2*	0 (0%)	50
	line 2 *exp.1*	0 (0%)	50
	line 2 *exp.2*	1 (2%)	50
	line 2 + Chl.	18 (36%)	50
day 10	line 1 *exp.1*	11 (24%)	46
	line 1 *exp.2*	7 (22%)	32
	line 2 *exp.1*	9 (18%)	50
	line 2 *exp.2*	6 (16%)	38

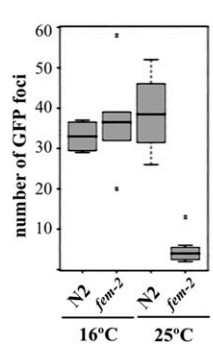

Figure 4 Protein aggregation in muscle of postreproductive worms. (A) Alkalinization of lysosomes in muscle cells of day 2 and day 10 wild-type animals expressing SEP::mCherry::LAAT-1. SEP fluorescence is quenched in acidic environments but detectable at pHs >6.5 (diagram on the right). Treatment with 200 mM of chloroquine leads to SEP-positive lysosomes in day 2. (B) Quantification of animals with lysosomal SEP signal in muscle cells. Two experiments (exp) with each of two independently generated transgenic lines (lines 1 and 2) were performed. (C) The *in situ* steady state of α-syn::GFP aggregates in muscle cells of wild-type (N2) and reproductively active (16°) or feminized (25°) *fem-2*(*b245ts*) day 6 worms. Insets are shown as grayscale/inverted images to highlight α-synuclein foci in black, denoted by arrowheads. (D) Quantification of α-syn::GFP foci (n = 20).

screen (Oh *et al.* 2006). To investigate whether DAF-16 mediates the lysosomal pH changes that occurred after the transition to postreproductive period, we first performed an *in silico* analysis of the 5′-upstream regions of v-ATPase genes in *C. elegans*. This analysis identified putative DAF-16 consensus binding sites (Murphy 2006) in 9 out of 20 *vha* genes (Figure S5A). To validate these genes as DAF-16 targets, we devised a native (noncrosslinking) ChIP protocol to circumvent the high background often associated with crosslinking used in conventional ChIP (see File S1). Using this assay, we recovered *vha-2*, *vha-8*, and *vha-17* among DAF-16 target genes (Figure 5C). Consistent with a role for DAF-16 as a transcriptional activator of the *vha* gene family, an RNAi knockdown of *daf-16* (corresponding to a 40% reduction in expression) resulted in a coordinated downregulation of *vha* gene transcription (Figure 5D) and a premature loss of lysosome acidity ($P < 0.0001$ by the Welch two sample t-test) in the intestine of actively reproducing worms (Figure 5E, quantified in Figure 5F).

The RNA analysis for *vha* genes suggested a diminished role for DAF-16-mediated transcription in the intestine during the transition to the postreproductive period. To directly examine this possibility, we followed individual worms expressing a transcriptional reporter for *mtl-2* (*Pmtl-2*::*GFP*), an intestinal metallothionein downregulated by DAF-16 (Bai *et al.* 2014). Relative to day 2, *Pmtl-2*::*GFP* fluorescence showed a remarkable increase by day 6, when reproduction is essentially over (Figure S4, B and C). We conclude that DAF-16 promotes v-ATPase activity and lysosomal pH by driving the expression of a subset of *vha* genes in the intestine (and

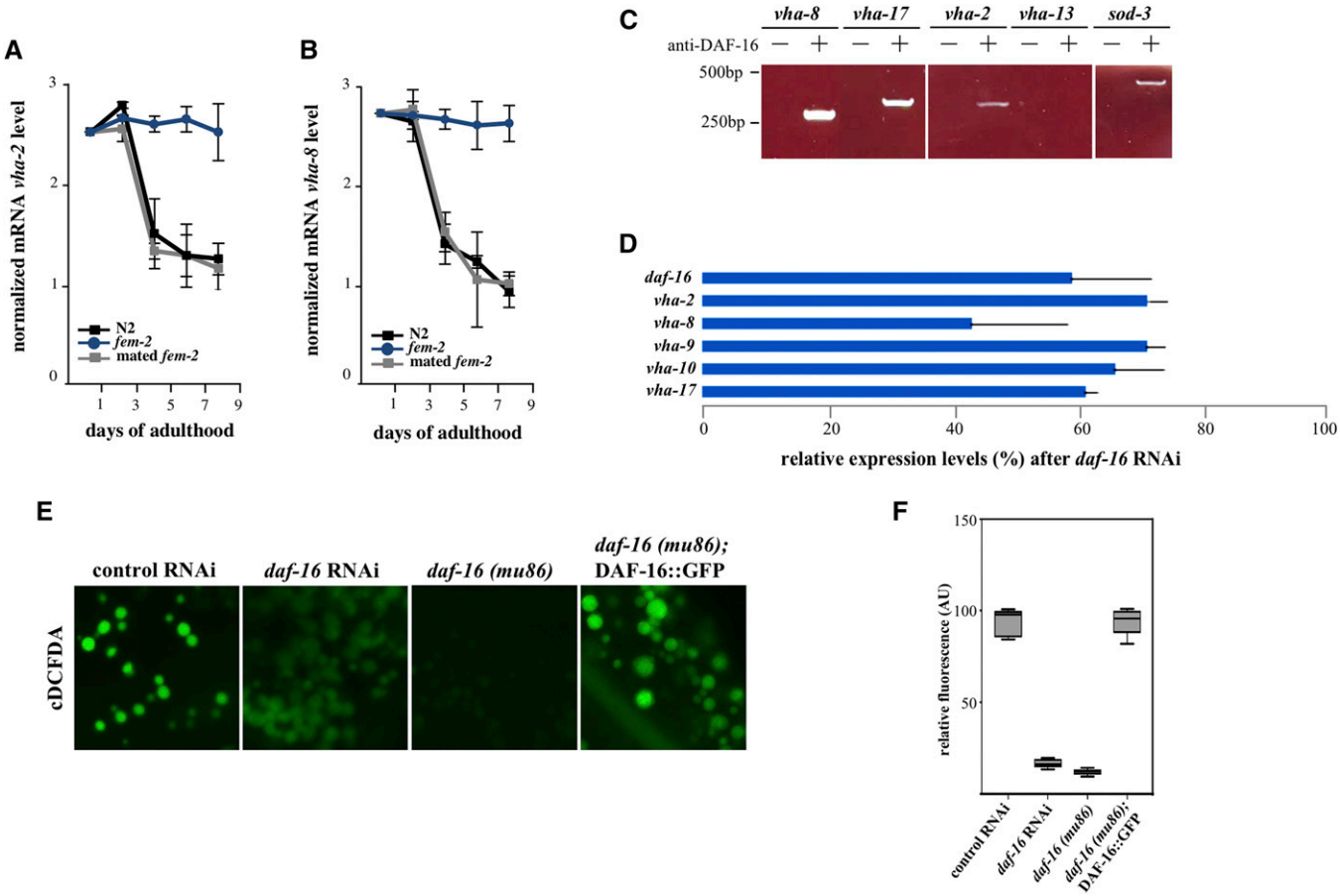

Figure 5 DAF-16 is a transcriptional activator of the *vha* gene family. (A, B) qRT-PCR analyses of *vha-2* and *vha-8* transcript levels in age-matched wild-type, feminized unmated, and feminized mated *fem-2* worms. RNA samples were analyzed in triplicate ($P < 0.0015$, two-tailed Student's *t*-test). (C) Binding of DAF-16 to *vha* gene promoters in day 2 wild-type worms assayed by ChIP. The known DAF-16 target gene *sod-3* (Murphy 2006) served as an experimental control. (D) Relative transcript levels of *vha* genes after a mild RNAi knockdown of *daf-16*. Two biological samples were analyzed in triplicate ($P < 0.005$, two-tailed Student's *t*-test). (E) Premature loss of acidity in intestinal lysosomes in reproductively active (day 2) worms after *daf-16* RNAi or in intestines of *daf-16*(*mu86*) mutants. Early lysosomal alkalinization is prevented in *daf-16* mutants expressing an integrated DAF-16::GFP transgene (*muIs61*). (F) Quantification of cDCFDA signal intensities for DAF-16-depleted animals, and in *daf-16* mutants expressing a DAF-16::GFP transgene (*muIs61*). The difference in signal loss between *daf-16* mutants and *daf-16* RNAi animals was not significant ($P = 0.0085$).

likely elsewhere) during progeny production, and that this activity is actively inhibited upon the end of reproduction.

In principle, the postreproductive reduction of *vha* transcripts in wild-type worms could be explained by a corresponding decrease in DAF-16 protein load in aging animals. We used a commercial polyclonal anti-DAF-16 antibody raised against its C-terminus to investigate whether native DAF-16 expression or localization in the intestine changes relative to the reproductive state. DAF-16 protein levels were comparable in lysates of days 2 and 10 from wild-type and *fem-2* worms (Figure S5B). However, in fixed intestines, native DAF-16 signals showed an age-dependent shift from the nucleus to the cytoplasm. While predominantly nuclear in reproducing wild-type (Figure 6A, quantified in Figure 6B), as well as in feminized, worms of the same age ($P = 0.9213$ by the Welch two sample *t*-test), DAF-16 was eventually excluded from the nuclei of wild-type worms transitioning to postreproductive period (days 6 and 8) while remaining mostly nuclear in older *fem-2* cells (Figure 6B, $P < 0.0001$ by the Welch two sample *t*-test). In comparison, no antibody signal was detected in intestines of *daf-16*(*mu86*) null mutants (Lin *et al.* 1997) (Figure S6A). The nuclear exclusion of DAF-16, timed with the cessation of progeny production, could explain the coordinated transcriptional downregulation of v-ATPase genes and the corresponding loss of lysosomal acidity in intestinal cells of postreproductive worms.

Studies tracking the dynamic changes in DAF-16 localization in live *C. elegans*, rather than fixed animals, have traditionally used overexpressed DAF-16 transgenes fused to fluorescent proteins. To validate the findings above, we identified a strain (HT1889) carrying an integrated *daf-16*::*gfp* construct with detectable intestinal signal in unstressed young animals and asked whether DAF-16::GFP subcellular localization was also subject to reproductive inputs. HT1889 animals express a DAF-16 isoform (DAF-16F) fused to GFP (*lpIs14*) that has been shown to respond to TOR signaling and regulate longevity in worms (Kwon *et al.* 2010). In live, young HT1889 adult animals, weak nuclear fluorescence in

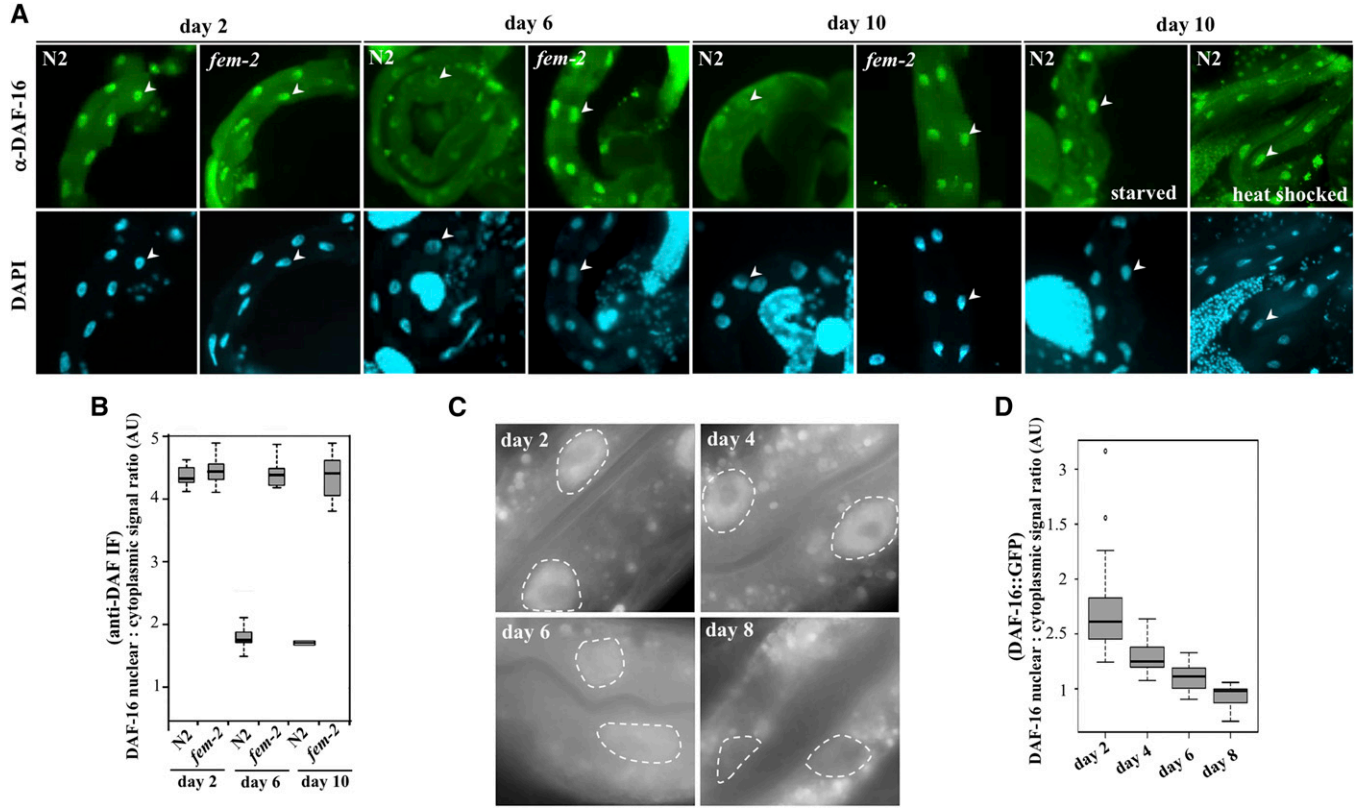

Figure 6 Exclusion of DAF-16 from the intestinal nuclei in postreproductive worms. (A) Immunostaining of dissected intestines of age-matched wild-type and sterile *fem-2* worms using a polyclonal anti-DAF-16 antibody. Worms were synchronized and processed for imaging in parallel. Nuclei are denoted by arrowheads. In parallel, we assayed DAF-16 nuclear localization in day 10 worms after a transient 40 min heat shock at 35°, or following an overnight growth on plates not supplemented with OP50. (B) Nuclear:cytoplasmic DAF-16 fluorescence signal ratios in intestinal cells of wild-type and *fem-2* worms. Mean ± SEM were scored for a minimum of 22 worms for each time point. (C) Representative images of *in vivo* intestinal cells expressing DAF-16F::GFP (*lpls14*), showing progressive loss of nuclear signal in day 6 and day 8 post-L4 animals. Nuclei are surrounded by dashed lines for visualization. (D) Quantification of nuclear:cytoplasmic ratios of DAF-16F::GFP signal intensity values. Measurements were taking using ImageJ from at least 10 different images each day.

the intestine was observed. Upon exiting the reproductive period (day 6 and 7), the nuclear DAF-16F::GFP signal in these cells faded (Figure 6C, quantified in Figure 6D). A similar age-dependent process is observed in yeast where the Forkheads Fkh1 and Fkh2 move out of the nucleus in chronologically aging cell populations (Postnikoff *et al.* 2012). The loss of DAF-16F::GFP nuclear signal postreproduction (day 8) is significant ($P < 0.0001$ by the Welch two sample *t*-test), though less abrupt than the one detected for the native DAF-16 (Figure 6, B and D). As others have noted, we did not observe significant accumulation of nuclear GFP signal in the intestine of live wild-type animals expressing three other DAF-16::GFP transgenes (*muIs61*, *xrIs87*, and *zIs356*) (Henderson and Johnson 2001; Lee *et al.* 2001; Lin *et al.* 2001; Wolf *et al.* 2008). However, it is noteworthy that, while DAF-16::GFP fluorescence in these strains are mostly cytoplasmic throughout adulthood in the intestine, *daf-16*(*mu86*); *muIs61* (DAF-16::GFP) animals (but not *mu86* worms) displayed a wild-type cDCFDA profile (Figure 5, E and F, $P = 0.8989$ by the Welch two sample *t*-test). This suggests that normally, a subset of intestinal DAF-16::GFP produced in these cells traffics to the nucleus at the peak of progeny production to sustain normal lysosomal pH in the intestine. Indeed, immunostaining of intestines from *daf-16*(*mu86*); *muIs61* [but not *daf-16*(*mu86*)] day 2 worms using the anti-DAF-16 antibody revealed nuclear staining in 35% ($n = 17$) of dissected animals (Figure S6B). Together, these results indicate that DAF-16 subcellular localization in the intestine is dynamically regulated during the transition from reproductive to postreproductive periods.

Several converging pathways regulate DAF-16 nuclear shuttling in response to metabolic and stress signals (Landis and Murphy 2010). Remarkably, a transient heat shock or nutritional deprivation restored DAF-16 nuclear localization in postreproductive animals (Figure 6A). The HSF-1-mediated heat stress response (Hsu *et al.* 2003), or the IGF-1-induced nutritional stress pathway (Lin *et al.* 2001) exert their effects in part by signaling DAF-16 nuclear localization. Induction of either pathway over-rides the effect of gonadal signaling on intestinal DAF-16 in postreproductive animals. These observations reveal the functional plasticity of DAF-16 in the intestine, and provide

further evidence of its nuclear recruitment via converging pathways.

Steroid signaling is required for acidic pH in intestinal lysosomes

In germ cell proliferation mutants, a signaling pathway composed in part of the nuclear hormone receptor DAF-12 (Antebi *et al.* 2000) and DAF-9/cytochrome P450, which catalyzes the synthesis of the lipophilic DAF-12-activating ligand Δ^4-dafachronic acid (DA) (Gerisch *et al.* 2001), augments the transcription of longevity genes by potentiating DAF-16 nuclear localization via the activity of KRI-1 (Berman and Kenyon 2006; Shen *et al.* 2012). The increase in lifespan triggered by loss of the germ cells requires the somatic gonad and intact steroid hormone signaling as mutations in *daf-12* or *daf-9* suppress the long-lived phenotype of germ cell proliferation mutants (Hsin and Kenyon 1999; Gerisch *et al.* 2001; Yamawaki *et al.* 2010). Furthermore, dietary supplementation with DA is sufficient to restore the expression of DAF-12 target genes in animals lacking the entire gonad (Gerisch *et al.* 2007; Yamawaki *et al.* 2010). DAF-9-mediated hormonal signaling is therefore required to delay somatic aging in animals lacking germ cells.

We examined a potential role for *daf-9/daf-12* signaling in regulating lysosomal pH. Similar to *daf-16* RNAi, a knockdown of *daf-12* also led to premature loss of lysosome acidity in the intestine of reproducing worms (Figure S7A, quantified in Figure S7B, $P < 0.0001$ by the Welch two sample *t*-test). Consistent with a role for hormonal signaling in sustaining somatic homeostasis, a *daf-9* mutation (*rh50*) accelerated the rise in pH in reproducing worms (Figure 7A). The removal of DAF-9-dependent signaling caused a similar premature alkalinization in lysosomes of young feminized (*fem-2*) worms (quantified in Figure 7B) mirrored by a significant increase ($P < 0.0001$ by the Welch two sample *t*-test) in the nuclear exclusion of DAF-16 in the intestine of these animals (Figure 7C, quantified in Figure 7D). The genetic requirement of *daf-9* for lysosomal acidification in *fem-2* worms can be bypassed by directly supplementing animals with DA (Figure 7E, quantified in Figure 7F). When *daf-9* or *fem-2*;*daf-9* worms were fed DA for 24 hr in early adulthood (day 1), levels of DAF-16 signal in the nuclei of intestinal cells significantly increased (Figure 7G, quantified in Figure 7H, $P < 0.0001$ by the Welch two sample *t*-test). These findings support a role for DAF-9-mediated hormonal signaling in the maintenance of lysosomal pH in the intestine via sustained nuclear DAF-16 localization.

Our results suggest that a hormonal signal is transduced to the intestine in a transient manner as a response to reproductive inputs from the gonad to maintain optimal lysosomal function during the period of maximal progeny production. Sterile mutants that fail to initiate fertilization in early adulthood escape early signs of somatic decay, presumably because of a defect in gonad to soma signaling. Reintroducing the ability to fertilize in these mutants, either by mating or growth at the permissive temperature, restores the normal rate of cellular deterioration in the soma as evidenced by changes in lysosomal pH (Figure 3A) and protein aggregation (Figure 4C), which may contribute to their shortened lifespan (Figure 3C). If the onset of protein aggregation in the soma of postreproductive worms is influenced by reduced hormonal signaling, DA supplementation alone should substitute for the lack of reproductive inputs at this life stage to delay lysosomal alkalinization. Indeed, worms fed DA continuously from L4 stage onwards displayed an acidic lysosomal profile (Figure 8A, quantified in Figure 8B, $P = 0.2218$) and DAF-16 nuclear localization at postreproductive stages that is more reminiscent of reproducing worms (Figure 8C, quantified in Figure 8D, $P = 0.259$ by the Welch two sample *t*-test).

Improved proteolysis in the soma leads to an extended period of sustained health (healthspan) during adult life by delaying the toxic effects of protein aggregation (Hahm *et al.* 2015). DA supplementation was associated with improved motility rates in postreproductive worms (Figure 8E), indicating that the overall impact of the gonad to soma signaling can be systemic. Similarly, we find that feminized *fem-2* mutants that also displayed a delay in lysosomal alkalinization in the intestine (Figure 3A) and less protein aggregation in muscle (Figure 4C), are notably more motile at older age than wild-type animals (File S2 and File S3), presumably because of sustained steroid hormone signaling. Taken together, these results decouple reproduction and lysosomal pH, and demonstrate that the pathway behind the gonad to soma signaling can be reactivated after the end of progeny production.

Discussion

A multitude of cellular and molecular changes permeate aging, responding to genetic and stochastic factors. Life history traits, such as reproduction, are important modulators of aging rates as seen by the evolutionary correspondence of different reproductive strategies in short- and long-lived species. In this context, decline in fertility is generally predictive of a rise in mortality rates (Jones *et al.* 2014). The current interpretation suggests that reproduction accelerates aging by depleting limited resources that otherwise could be used by the soma (Kirkwood and Austad 2000). To achieve the optimal balance between longevity and reproduction, the reproductive capacity in the gonad must be somehow relayed to the rest of the organism through signaling pathways reaching across tissues. Evidence from *C. elegans* mutants with disrupted germ cell proliferation indicates that active signaling from the gonad to the soma depends on the DAF-9/DAF-12 steroid hormone signaling pathway that converges on DAF-16 activity (Kenyon 2010a). Our results suggest that steroid signaling also controls homeostasis in the soma of reproducing worms. An *in silico* analysis revealed a marked downregulation of *daf-9* mRNA coincident with the end of reproduction in wild-type hermaphrodites (Figure S8) (Lund *et al.* 2002). Unlike *daf-9*, many of the genes intrinsic to or preferentially expressed in germ cells, including a family of

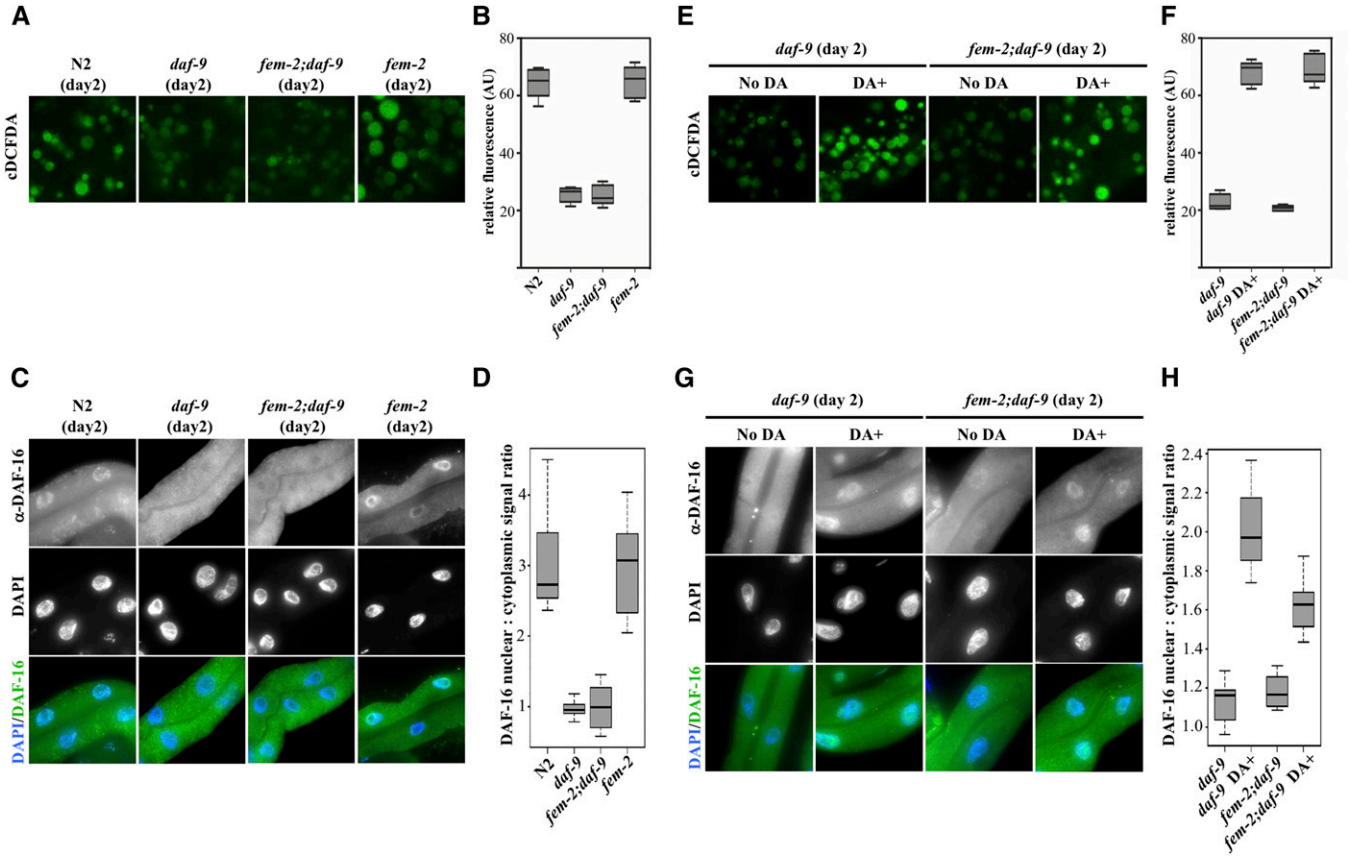

Figure 7 DAF-9 mediates the delay in pH alkalinization in *fem-2* mutants. (A) Premature loss of acidity in intestinal lysosomes of young (day 2) *daf-9* (*rh50*) and feminized *fem-2*;*daf-9* mutants. (B) Quantification of cDCFDA signal intensities in day 2 wild-type, *daf-9*, *fem-2* and *fem-2*;*daf-9* worms. (C) Immunostaining of DAF-16 in intestines of day 2 of wild-type, *daf-9*, *fem-2*, and *fem-2*;*daf-9* worms. (D) Nuclear:cytoplasmic DAF-16 fluorescence signal ratios in intestinal cells of day 2 of wild-type, *daf-9*, *fem-2*, and *fem-2*;*daf-9*. Depletion of *daf-9* in a feminized *fem-2* background results in premature loss of DAF-16 nuclear signal to *daf-9* mutant levels (P value $<$ 0.0001 by the Welch two sample t-test). (E) Supplementation with 10 μM DA rescues the defects in lysosomal acidification in *daf-9* mutants. (F) Quantification of cDCFDA signal intensities in day 2 of *daf-9* and *fem-2*;*daf-9* animals with and without 10 μM DA supplementation. (G) Immunostaining of DAF-16 in intestines of day 2 *daf-9* and *fem-2*;*daf-9* worms with and without 10 μM DA supplementation. DA significantly increases DAF-16 nuclear signal levels in *daf-9* and *fem-2*;*daf-9* animals (P $<$ 0.0001 by the Welch two sample t-test). (H) Nuclear:cytoplasmic DAF-16 fluorescence signal ratios in intestinal cells of day 2 of *daf-9* and *fem-2*;*daf-9* animals with and without 10 μM DA supplementation.

piwi-related genes that regulate germ cell proliferation and development (Reinke *et al.* 2000; Lund *et al.* 2002) maintained or displayed increased expression immediately past the reproductive period (days 6–11). Cessation of reproduction in worms, therefore, does not appear to be accompanied with a general decline of the gonadal transcriptional network—an observation corroborated by the capacity to cross-fertilize hermaphrodites long after sperm depletion (Hodgkin and Barnes 1991). We propose that, as in germ-cell-depleted worms (Hsin and Kenyon 1999; Antebi *et al.* 2000; Gerisch *et al.* 2001; Shen *et al.* 2012), this signaling pathway co-opts sterol compound biosynthesis in order to transduce the reproductive cues from the gonads to the soma (Figure 9). Two important aspects concerning the mechanistic induction of this pathway remain to be elucidated. First, does a shut off of *daf-9* expression in the gonads after reproduction translate to reduced *daf-12/daf-16* signaling? And second, how do worms signal the end of reproduction?

Our results show that mutants that fail to reproduce, either due to a lack of germ cell proliferation or sperm production, show a youthful profile of lysosomal acidity at older age and improved protein clearance. Normal alkalinization of intestinal lysosomes requires, therefore, passage through the reproductive cycle. In this interpretation, the decrease in progeny generation that marks the end of reproductive life must be perceived by the gonad to inhibit the synthesis of steroid ligands. This shut off mechanism is prevented in young reproducing worms via a signal originated from sperm or fertilized oocyte. As the supply of sperm cells is exhausted and fertilization dwindles, diminished signaling from the gonad would eventually release steroid synthesis inhibition, resulting in reduced DAF-16 activation in the intestine. In our model (Figure 9), this coincides with the short window of time in late reproductive life when loss of acidity is first observed in lysosomes. We propose that sterile animals that fail to enter the reproductive cycle somehow bypass the

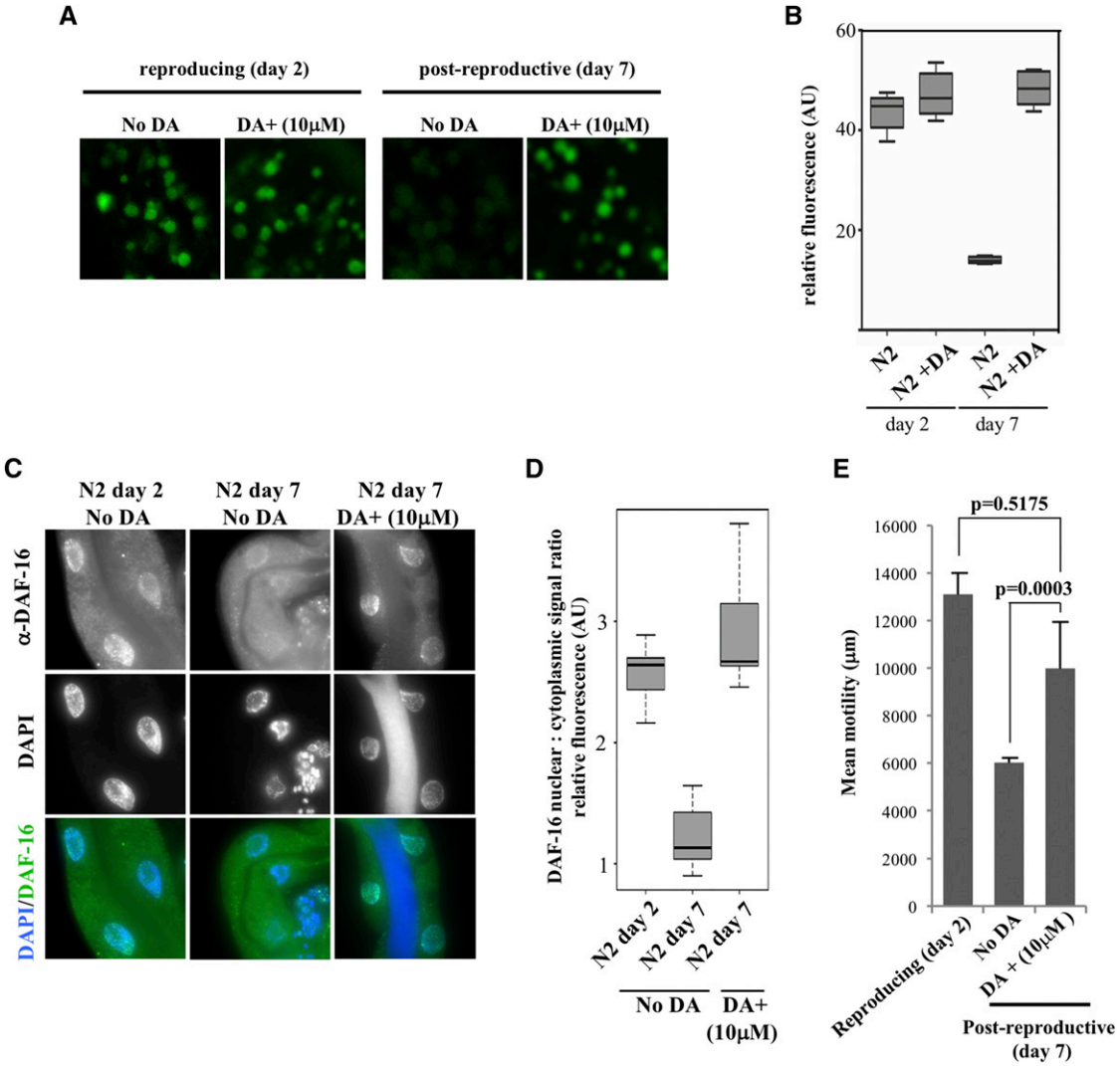

Figure 8 DA supplementation is sufficient to sustain acidic lysosomes in postreproductive worms. Comparison of reproductive (day 2) and postreproductive (day 7) wild-type worms that have been supplemented with different concentration of DA or just the vehicle (ethanol). (A) cDCFDA profiles. (B) Quantification of cDCFDA signal intensities. (C) Immunostaining of intestinal DAF-16 in controls or animals fed DA. (D) Nuclear:cytoplasmic DAF-16 fluorescence signal ratios in intestines. Constitutive DA feeding significantly increases nuclear DAF-16 levels in postreproductive wild-type worms when compared non-DA fed controls ($P < 0.0001$ by the Welch two sample *t*-test). (E) The effect of DA supplementation in the motility of reproducing and postreproductive worms. One minute movies of three worms for each treatment were recorded in a worm tracker system (MBF Bioscience), and the movement of worms on an agar plate tracked using WormLab. *P* values were calculated using the Welch two sample *t*-test.

inhibition of steroid ligand production thereby avoiding the normal wave of lysosomal alkalinization. Under this interpretation, gonads signal the transition between fertile and nonfertile periods to delineate the temporal boundaries of progeny generation to nonreproductive tissues.

Mechanistically, enhanced lysosomal function via the upregulation of v-ATPase transcription has been previously shown to contribute to the lifespan extension observed in *glp-1* worms (Lapierre *et al.* 2013). Similar to *glp-1* (Lin *et al.* 2001), self-sterile mutants such as *fog-2*, *fem-1*;*rrf-3* (Miyata *et al.* 2008), and *fem*-2 (this study) also display nuclear DAF-16 during adulthood. In *fog-2* animals, nuclear DAF-16 in the intestine is licensed by the lack of an inhibitory signal normally coming from the early embryo leading to a DAF-16-dependent pathogen-resistant phenotype (Miyata *et al.* 2008). Abrogating reproduction in *fem-1* animals results in a marked reduction in the expression of vitellogenins (*vit* genes). Vitellogenin gene transcription is required for yolk synthesis in the intestine, a process with an associated higher energetic cost for the animal and normally inhibited by DAF-16 (DePina *et al.* 2011). Suppression of vitellogenesis, on the other hand, has been linked to increases in lifespan through DAF-16 activation (Murphy *et al.* 2003; Kenyon 2010b). As with lysosomal pH (this study), reinstating reproduction in self-sterile mutants through mating prevents the drop in *vit* transcription (Miyata *et al.* 2008), and suppresses resistance to *P. aeruginosa* infection (DePina *et al.* 2011), presumably as a result of DAF-16 nuclear exclusion. These studies point to a

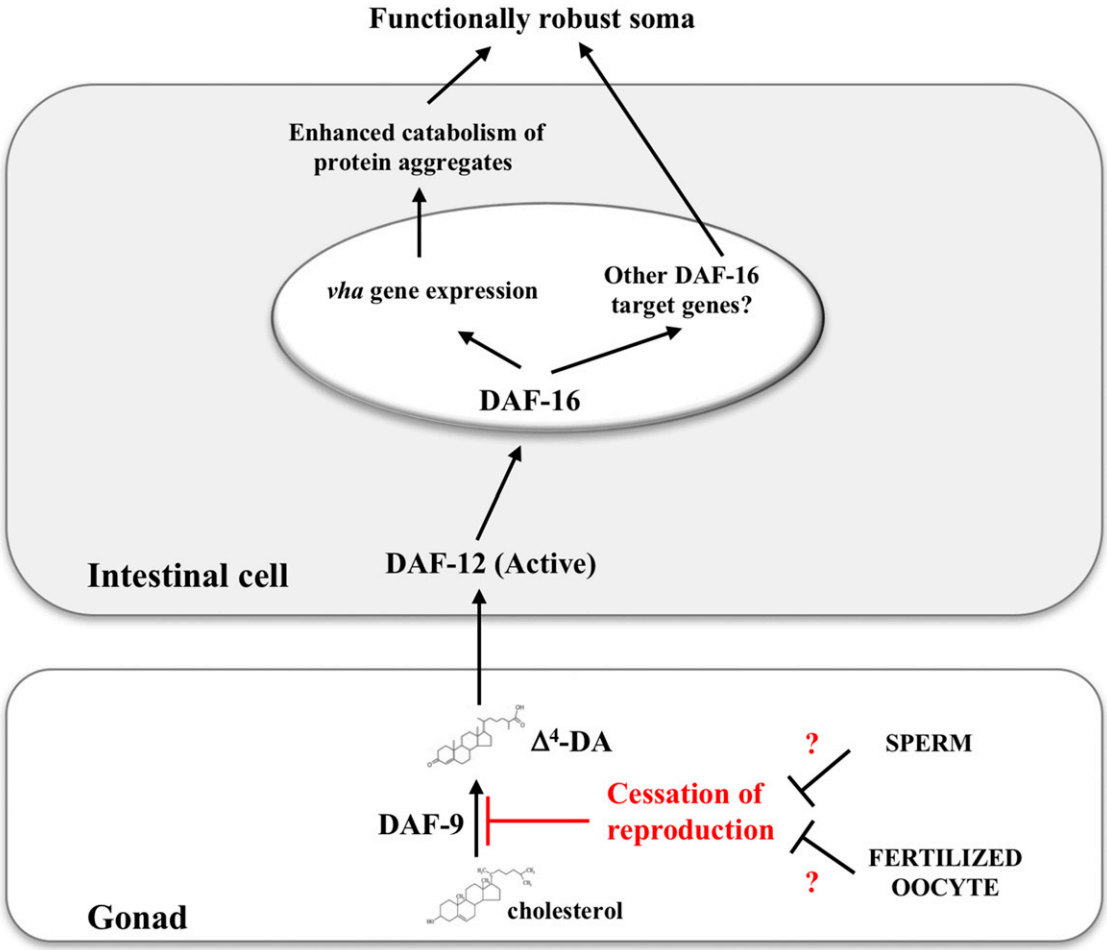

Figure 9 A hormonal signaling pathway that functionally couples the soma to the gonad in progeny producing worms. A signaling pathway that couples somatic homeostasis to the reproduction state in the gonads. In reproducing worms, biosynthesis of the sterol ligand DA by DAF-9 transduces a longevity signal from the gonads to the soma by activating the nuclear hormone receptor DAF-12, which, in turn, augments the transcriptional induction of longevity-promoting genes by potentiating DAF-16 nuclear localization.

general increase in DAF-16 activity in sterile backgrounds, with and without germ cells, and suggest that lifespan could be impacted as a consequence. Indeed, we find that as reported for *glp-1* and *spe-26* animals (Gems and Riddle 1996; Arantes-Oliveira *et al.* 2002), *fem-2* mutants also live longer than the wild type (Figure 3C). However, other self-sterile mutants including *fem-1* and *fog-2* have been shown to have normal longevity, despite their DAF-16 nuclear localization (Arantes-Oliveira *et al.* 2002; Miyata *et al.* 2008). Considering the complexity in transcriptional outcomes resulted from DAF-16 activation (Libina *et al.* 2003), it will be important to determine if other feminized mutants also show prolonged lysosomal acidification. New approaches to evaluate the global impact of mutations in aging-related processes take advantages of changes in healthspan, which focuses on specific functional declines, such as diminished movement. Mutations that improve how animals age do not necessarily alter lifespan in isolation, though mutants that show increased lifespan often do so by affecting multiple healthspan variables (Tissenbaum 2012). We found that *fem-2* females, which showed reduced age-dependent protein aggregation in muscle cells (Figure 4C and Figure S2C), were also more active in later life stages than their age matched wild-type counterpart, an effect that could be phenocopied in postreproductive wild-type worms by supplementation with DA (Figure 8E, File S2, and File S3). To determine how broadly reproduction affects fitness, it will be necessary to test other self-sterile mutants with wild-type lifespan for changes in healthspan.

We have implicated nuclear shuttling of DAF-16 in maintaining the acidity of intestinal lysosomes during the progeny producing period via the upregulation of v-ATPase transcription. Transactivation of v-ATPase genes in specialized epithelia of mouse also requires a Forkhead transcription factor (Foxi1) to promote lumen acidification in the inner ear, epididymis and kidney (Vidarsson *et al.* 2009). We find that, in *C. elegans*, the end of progeny generation is accompanied by a reduction of nuclear DAF-16 signals in the intestine at a time when age-related tissue decline is observed. Downregulation of DAF-16-mediated transcription correlates with age-dependent

nuclear exclusion of DAF-16 and contributes to normal aging in C. *elegans* (Tepper *et al.* 2013). In our analysis, the drop in nuclear DAF-16 signals corresponded with a reduction in v-ATPase gene expression that anticipated a loss of lysosomal acidity in the intestine of postreproductive *C. elegans* (Figure 2A, Figure 5, A and B, and Figure S4, A and C). An age-dependent decrease in *vha-6* transcripts in the *C. elegans* intestine, and a global loss of v-ATPase in aged human cortex have been previously reported (Lu *et al.* 2004; Adamla and Ignatova 2015). Furthermore, the alkalinization in vacuoles of aging fission yeast cells can be prevented by overexpressing the v-ATPase subunit *vma1*, while depletion of v-ATPase leads to a shortening in chronological lifespan (Stephan *et al.* 2013). Thus, loss of v-ATPase activity appears to be a common signature of aging cells across different species. In a complementary study, we describe the involvement of *S. cerevisae* Forkhead proteins in regulating the expression of v-ATPase (*vma*) genes (A.G. *et al.*, unpublished data). In young yeast cells, the Fox protein Hcm1 upregulates Fkh1 and Fkh2 transcription, which, in turn mediate expression of several *vma* gene family members. Upon the end of replicative life, Hcm1 is relocalized to the cytoplasm, and Fkh1 and Fkh2 expression reduced as a consequence. Loss of Fkh proteins, as with DAF-16 nuclear exclusion, negatively impacts v-ATPase production leading to vacuolar alkalinization in old yeast cells. Similar to worms, this is temporally marked by the increase in protein aggregation, and followed by senescence. These results reveal that the recruitment of Forkheads to actively regulate proteostasis through maintenance of lysosomal pH is an evolutionary conserved and ancient pathway that precedes multicellularity and the consequent rise of the germ-soma conflict for limited resources. We propose that loss of lysosomal acidity may serve as a new biomarker of aging in worms, and offer a testable model for how cessation of reproduction may be coupled to somatic breakdown. Significantly, our studies suggest that the rise in lysosomal pH is not a stochastic consequence of aging, but rather, it is sensitive to the reproductive cycle. In mutants in which reproduction is abrogated, acidified lysosomes persisted in adult life, delaying the formation of protein aggregation. A key prediction of these findings is that restoring the reproductive cycle in these mutants should trigger lysosomal alkalinization. In line with this idea, mating suppressed the extended lysosomal acidification phenotype in feminized animals (Figure 3A). In this model, prolonged expression and activity of Forkhead proteins promotes homeostasis through the maintenance of lysosomal acidification.

How does lysosomal alkalinization contribute to aging? A ubiquitous feature of eukaryotic aging is the progressive formation of misfolded and irreversibly modified proteins in old cells (Yin 1996; Brunk and Terman 2002b; Arrasate *et al.* 2004; Gerland *et al.* 2004; Poon *et al.* 2006; Erjavec *et al.* 2007). Aggregation-prone proteins accumulate in the lysosomal lumen of old worms. This cytological feature is similar to the appearance of lipofuscin, a heterogeneous mix of oxidized/cross linked proteins, in the lysosomes of late passage mammalian cultured cells (Yin 1996; Gerland *et al.* 2004). Lysosomes represent the biological end point of the cellular catabolic machinery. The continuous influx of proteins into alkalinized lysosomes may result in the functional collapse of these organelles, loss of cellular catabolism in the soma, and, ultimately, senescence. Alternatively, deterioration of lysosomal function could also impact aging by disrupting signaling pathways that require passage through the lysosome. For instance, lysosomes in *C. elegans* have recently been shown to promote longevity by enabling the activation of the nuclear receptors NHR-49 and NHR-80, required for normal lifespan (Folick *et al.* 2015).

Acknowledgments

We thank G.A. Caldwell and the *Caenorhabditis Genetics Center* (CGC) [National Institutes of Health (NIH) grant P40OD010440] for providing strains. We acknowledge A. Almousa for help with qPCR data analysis and G. Liu for help with confocal microscopy. This work was supported by grants from the Natural Sciences and Engineering Research Council of Canada (NSERC) and Innovation Canada.

Literature Cited

Adamla, F., and Z. Ignatova, 2015 Somatic expression of unc-54 and vha-6 mRNAs declines but not pan-neuronal rgef-1 and unc-119 expression in aging Caenorhabditis elegans. Sci. Rep. 5: 10692.

Ahlberg, J., A. Berkenstam, F. Henell, and H. Glaumann, 1985 Degradation of short and long lived proteins in isolated rat liver lysosomes. Effects of pH, temperature, and proteolytic inhibitors. J. Biol. Chem. 260: 5847–5854.

Antebi, A., 2013 Regulation of longevity by the reproductive system. Exp. Gerontol. 48: 596–602.

Antebi, A., W. H. Yeh, D. Tait, E. M. Hedgecock, and D. L. Riddle, 2000 daf-12 encodes a nuclear receptor that regulates the dauer diapause and developmental age in C. elegans. Genes Dev. 14: 1512–1527.

Arantes-Oliveira, N., J. Apfeld, A. Dillin, and C. Kenyon, 2002 Regulation of life-span by germ-line stem cells in Caenorhabditis elegans. Science 295: 502–505.

Arrasate, M., S. Mitra, E. S. Schweitzer, M. R. Segal, and S. Finkbeiner, 2004 Inclusion body formation reduces levels of mutant huntingtin and the risk of neuronal death. Nature 431: 805–810.

Bai, Y., D. Zhi, C. Li, D. Liu, J. Zhang *et al.*, 2014 Infection and immune response in the nematode Caenorhabditis elegans elicited by the phytopathogen Xanthomonas. J. Microbiol. Biotechnol. 24: 1269–1279.

Ben-Zvi, A., E. A. Miller, and R. I. Morimoto, 2009 Collapse of proteostasis represents an early molecular event in Caenorhabditis elegans aging. Proc. Natl. Acad. Sci. USA 106: 14914–14919.

Berman, J. R., and C. Kenyon, 2006 Germ-cell loss extends C. elegans life span through regulation of DAF-16 by kri-1 and lipophilic-hormone signaling. Cell 124: 1055–1068.

Boulias, K., and H. R. Horvitz, 2012 The C. elegans microRNA mir-71 acts in neurons to promote germline-mediated longevity through regulation of DAF-16/FOXO. Cell Metab. 15: 439–450.

Boya, P., 2012 Lysosomal function and dysfunction: mechanism and disease. Antioxid. Redox Signal. 17: 766–774.

Brunk, U. T., and A. Terman, 2002a Lipofuscin: mechanisms of age-related accumulation and influence on cell function. Free Radic. Biol. Med. 33: 611–619.
Brunk, U. T., and A. Terman, 2002b The mitochondrial-lysosomal axis theory of aging: accumulation of damaged mitochondria as a result of imperfect autophagocytosis. Eur. J. Biochem. 269: 1996–2002.
Burkewitz, K., K. P. Choe, E. C. Lee, A. Deonarine, and K. Strange, 2012 Characterization of the proteostasis roles of glycerol accumulation, protein degradation and protein synthesis during osmotic stress in C. elegans. PLoS One 7: e34153.
Cargill, S. L., J. R. Carey, H. G. Muller, and G. Anderson, 2003 Age of ovary determines remaining life expectancy in old ovariectomized mice. Aging Cell 2: 185–190.
Clokey, G. V., and L. A. Jacobson, 1986 The autofluorescent "lipofuscin granules" in the intestinal cells of Caenorhabditis elegans are secondary lysosomes. Mech. Ageing Dev. 35: 79–94.
Cohen, E., J. Bieschke, R. M. Perciavalle, J. W. Kelly, and A. Dillin, 2006 Opposing activities protect against age-onset proteotoxicity. Science 313: 1604–1610.
Colacurcio, D. J., and R. A. Nixon, 2016 Disorders of lysosomal acidification-the emerging role of v-ATPase in aging and neurodegenerative disease. Ageing Res. Rev. 32: 75–88.
Cuervo, A. M., and J. F. Dice, 2000 When lysosomes get old. Exp. Gerontol. 35: 119–131.
Cuervo, A. M., E. Bergamini, U. T. Brunk, W. Droge, M. Ffrench *et al.*, 2005 Autophagy and aging: the importance of maintaining "clean" cells. Autophagy 1: 131–140.
David, D. C., N. Ollikainen, J. C. Trinidad, M. P. Cary, A. L. Burlingame *et al.*, 2010 Widespread protein aggregation as an inherent part of aging in C. elegans. PLoS Biol. 8: e1000450.
DePina, A. S., W. B. Iser, S. S. Park, S. Maudsley, M. A. Wilson *et al.*, 2011 Regulation of Caenorhabditis elegans vitellogenesis by DAF-2/IIS through separable transcriptional and posttranscriptional mechanisms. BMC Physiol. 11: 11.
DiLoreto, R., and C. T. Murphy, 2015 The cell biology of aging. Mol. Biol. Cell 26: 4524–4531.
Duvvuri, M., Y. Gong, D. Chatterji, and J. P. Krise, 2004 Weak base permeability characteristics influence the intracellular sequestration site in the multidrug-resistant human leukemic cell line HL-60. J. Biol. Chem. 279: 32367–32372.
Erjavec, N., L. Larsson, J. Grantham, and T. Nystrom, 2007 Accelerated aging and failure to segregate damaged proteins in Sir2 mutants. Genes Dev. 21: 2410–2421.
Farkas, R., D. Benova-Liszekova, L. Mentelova, S. Mahmood, Z. Datkova *et al.*, 2015 Vacuole dynamics in the salivary glands of Drosophila melanogaster during prepupal development. Dev. Growth Differ. 57: 74–96.
Flatt, T., K. J. Min, C. D'Alterio, E. Villa-Cuesta, J. Cumbers *et al.*, 2008 Drosophila germ-line modulation of insulin signaling and lifespan. Proc. Natl. Acad. Sci. USA 105: 6368–6373.
Folick, A., H. D. Oakley, Y. Yu, E. H. Armstrong, M. Kumari *et al.*, 2015 Aging. Lysosomal signaling molecules regulate longevity in Caenorhabditis elegans. Science 347: 83–86.
Gems, D., and D. L. Riddle, 1996 Longevity in Caenorhabditis elegans reduced by mating but not gamete production. Nature 379: 723–725.
Gerisch, B., C. Weitzel, C. Kober-Eisermann, V. Rottiers, and A. Antebi, 2001 A hormonal signaling pathway influencing C. elegans metabolism, reproductive development, and life span. Dev. Cell 1: 841–851.
Gerisch, B., V. Rottiers, D. Li, D. L. Motola, C. L. Cummins *et al.*, 2007 A bile acid-like steroid modulates Caenorhabditis elegans lifespan through nuclear receptor signaling. Proc. Natl. Acad. Sci. USA 104: 5014–5019.
Gerland, L. M., L. Genestier, S. Peyrol, M. C. Michallet, S. Hayette *et al.*, 2004 Autolysosomes accumulate during in vitro CD8+ T-lymphocyte aging and may participate in induced death sensitization of senescent cells. Exp. Gerontol. 39: 789–800.
Ghavidel, A., K. Baxi, V. Ignatchenko, M. Prusinkiewicz, T. G. Arnason *et al.*, 2015 A Genome scale screen for mutants with delayed exit from mitosis: Ire1-independent induction of autophagy integrates ER homeostasis into mitotic lifespan. PLoS Genet. 11: e1005429.
Ghazi, A., S. Henis-Korenblit, and C. Kenyon, 2009 A transcription elongation factor that links signals from the reproductive system to lifespan extension in Caenorhabditis elegans. PLoS Genet. 5: e1000639.
Golden, T. R., and S. Melov, 2004 Microarray analysis of gene expression with age in individual nematodes. Aging Cell 3: 111–124.
Hahm, J. H., S. Kim, R. DiLoreto, C. Shi, S. J. Lee *et al.*, 2015 C. elegans maximum velocity correlates with healthspan and is maintained in worms with an insulin receptor mutation. Nat. Commun. 6: 8919.
Harrington, A. J., A. L. Knight, G. A. Caldwell, and K. A. Caldwell, 2011 Caenorhabditis elegans as a model system for identifying effectors of alpha-synuclein misfolding and dopaminergic cell death associated with Parkinson's disease. Methods 53: 220–225.
Harrison, T. S., J. Chen, E. Simons, and S. M. Levitz, 2002 Determination of the pH of the Cryptococcus neoformans vacuole. Med. Mycol. 40: 329–332.
Henderson, S. T., and T. E. Johnson, 2001 daf-16 integrates developmental and environmental inputs to mediate aging in the nematode Caenorhabditis elegans. Curr. Biol. 11: 1975–1980.
Hermann, G. J., L. K. Schroeder, C. A. Hieb, A. M. Kershner, B. M. Rabbitts *et al.*, 2005 Genetic analysis of lysosomal trafficking in Caenorhabditis elegans. Mol. Biol. Cell 16: 3273–3288.
Herndon, L. A., P. J. Schmeissner, J. M. Dudaronek, P. A. Brown, K. M. Listner *et al.*, 2002 Stochastic and genetic factors influence tissue-specific decline in ageing C. elegans. Nature 419: 808–814.
Ho, C. Y., C. H. Choy, C. A. Wattson, D. E. Johnson, and R. J. Botelho, 2015 The Fab1/PIKfyve phosphoinositide phosphate kinase is not necessary to maintain the pH of lysosomes and of the yeast vacuole. J. Biol. Chem. 290: 9919–9928.
Hodgkin, J., and T. M. Barnes, 1991 More is not better: brood size and population growth in a self-fertilizing nematode. Proc. Biol. Sci. 246: 19–24.
Holmberg, C. I., K. E. Staniszewski, K. N. Mensah, A. Matouschek, and R. I. Morimoto, 2004 Inefficient degradation of truncated polyglutamine proteins by the proteasome. EMBO J. 23: 4307–4318.
Horn, M. A., R. P. Meadows, I. Apostol, C. R. Jones, D. G. Gorenstein *et al.*, 1992 Effect of elicitation and changes in extracellular pH on the cytoplasmic and vacuolar pH of suspension-cultured soybean cells. Plant Physiol. 98: 680–686.
Hsin, H., and C. Kenyon, 1999 Signals from the reproductive system regulate the lifespan of C. elegans. Nature 399: 362–366.
Hsu, A. L., C. T. Murphy, and C. Kenyon, 2003 Regulation of aging and age-related disease by DAF-16 and heat-shock factor. Science 300: 1142–1145.
Hughes, A. L., and D. E. Gottschling, 2012 An early age increase in vacuolar pH limits mitochondrial function and lifespan in yeast. Nature 492: 261–265.
Hughes, S. E., K. Evason, C. Xiong, and K. Kornfeld, 2007 Genetic and pharmacological factors that influence reproductive aging in nematodes. PLoS Genet. 3: e25.
Hutter, H., and R. Schnabel, 1994 glp-1 and inductions establishing embryonic axes in C. elegans. Development 120: 2051–2064.
Jones, O. R., A. Scheuerlein, R. Salguero-Gomez, C. G. Camarda, R. Schaible *et al.*, 2014 Diversity of ageing across the tree of life. Nature 505: 169–173.
Kenyon, C., 2005 The plasticity of aging: insights from long-lived mutants. Cell 120: 449–460.
Kenyon, C., 2010a A pathway that links reproductive status to lifespan in Caenorhabditis elegans. Ann. N. Y. Acad. Sci. 1204: 156–162.

Kenyon, C. J., 2010b The genetics of ageing. Nature 464: 504–512.
Kim, D. K., H. S. Lim, I. Kawasaki, Y. H. Shim, N. N. Vaikath *et al.*, 2016 Anti-aging treatments slow propagation of synucleinopathy by restoring lysosomal function. Autophagy 12: 1849–1863.
Kimble, J., and S. L. Crittenden, 2005 Germline proliferation and its control (August 15, 2005), Wormbook, ed. The *C. elegans* Research Community WormBook, doi/10.1895/wormbook.1.13.1, http://wormbook.org.
Kirkwood, T. B., 1977 Evolution of ageing. Nature 270: 301–304.
Kirkwood, T. B., and S. N. Austad, 2000 Why do we age? Nature 408: 233–238.
Kosegarten, H., F. Grolig, J. Wieneke, G. Wilson, and B. Hoffmann, 1997 Differential ammonia-elicited changes of cytosolic pH in root hair cells of rice and maize as monitored by 2[prime], 7[prime]-bis-(2-carboxyethyl)-5 (and -6)-carboxyfluorescein-fluorescence ratio. Plant Physiol. 113: 451–461.
Kwon, E. S., S. D. Narasimhan, K. Yen, and H. A. Tissenbaum, 2010 A new DAF-16 isoform regulates longevity. Nature 466: 498–502.
Labbadia, J., and R. I. Morimoto, 2015 Repression of the heat shock response is a programmed event at the onset of reproduction. Mol. Cell 59: 639–650.
Landis, J. N., and C. T. Murphy, 2010 Integration of diverse inputs in the regulation of Caenorhabditis elegans DAF-16/FOXO. Dev. Dyn. 239: 1405–1412.
Lapierre, L. R., C. D. De Magalhaes Filho, P. R. McQuary, C. C. Chu, O. Visvikis *et al.*, 2013 The TFEB orthologue HLH-30 regulates autophagy and modulates longevity in Caenorhabditis elegans. Nat. Commun. 4: 2267.
Lee, R. Y., J. Hench, and G. Ruvkun, 2001 Regulation of C. elegans DAF-16 and its human ortholog FKHRL1 by the daf-2 insulin-like signaling pathway. Curr. Biol. 11: 1950–1957.
Lee, S. K., W. Li, S. E. Ryu, T. Rhim, and J. Ahnn, 2010 Vacuolar (H+)-ATPases in Caenorhabditis elegans: what can we learn about giant H+ pumps from tiny worms? Biochim. Biophys. Acta 1797: 1687–1695.
Levitte, S., R. Salesky, B. King, S. Coe Smith, M. Depper *et al.*, 2010 A Caenorhabditis elegans model of orotic aciduria reveals enlarged lysosome-related organelles in embryos lacking umps-1 function. FEBS J. 277: 1420–1439.
Li, J., M. Tewari, M. Vidal, and S. S. Lee, 2007 The 14–3-3 protein FTT-2 regulates DAF-16 in Caenorhabditis elegans. Dev. Biol. 301: 82–91.
Li, Y., B. Chen, W. Zou, X. Wang, Y. Wu *et al.*, 2016 The lysosomal membrane protein SCAV-3 maintains lysosome integrity and adult longevity. J. Cell Biol. 215: 167–185.
Liang, V., M. Ullrich, H. Lam, Y. L. Chew, S. Banister *et al.*, 2014 Altered proteostasis in aging and heat shock response in C. elegans revealed by analysis of the global and de novo synthesized proteome. Cell. Mol. Life Sci. 71: 3339–3361.
Libina, N., J. R. Berman, and C. Kenyon, 2003 Tissue-specific activities of C. elegans DAF-16 in the regulation of lifespan. Cell 115: 489–502.
Lim, C. Y., and R. Zoncu, 2016 The lysosome as a command-and-control center for cellular metabolism. J. Cell Biol. 214: 653–664.
Lin, K., J. B. Dorman, A. Rodan, and C. Kenyon, 1997 daf-16: an HNF-3/forkhead family member that can function to double the life-span of Caenorhabditis elegans. Science 278: 1319–1322.
Lin, K., H. Hsin, N. Libina, and C. Kenyon, 2001 Regulation of the Caenorhabditis elegans longevity protein DAF-16 by insulin/IGF-1 and germline signaling. Nat. Genet. 28: 139–145.
Liu, B., H. Du, R. Rutkowski, A. Gartner, and X. Wang, 2012 LAAT-1 is the lysosomal lysine/arginine transporter that maintains amino acid homeostasis. Science 337: 351–354.
Liu, J., B. Zhang, H. Lei, Z. Feng, J. Liu *et al.*, 2013 Functional aging in the nervous system contributes to age-dependent motor activity decline in C. elegans. Cell Metab. 18: 392–402.
Lu, T., Y. Pan, S. Y. Kao, C. Li, I. Kohane *et al.*, 2004 Gene regulation and DNA damage in the ageing human brain. Nature 429: 883–891.
Lund, J., P. Tedesco, K. Duke, J. Wang, S. K. Kim *et al.*, 2002 Transcriptional profile of aging in C. elegans. Curr. Biol. 12: 1566–1573.
Luo, S., G. A. Kleemann, J. M. Ashraf, W. M. Shaw, and C. T. Murphy, 2010 TGF-beta and insulin signaling regulate reproductive aging via oocyte and germline quality maintenance. Cell 143: 299–312.
Madeo, F., T. Eisenberg, and G. Kroemer, 2009 Autophagy for the avoidance of neurodegeneration. Genes Dev. 23: 2253–2259.
McGee, M. D., D. Weber, N. Day, C. Vitelli, D. Crippen *et al.*, 2011 Loss of intestinal nuclei and intestinal integrity in aging C. elegans. Aging Cell 10: 699–710.
Mello, C., and A. Fire, 1995 DNA transformation. Methods Cell Biol. 48: 451–482.
Miyata, S., J. Begun, E. R. Troemel, and F. M. Ausubel, 2008 DAF-16-dependent suppression of immunity during reproduction in Caenorhabditis elegans. Genetics 178: 903–918.
Mohri-Shiomi, A., and D. A. Garsin, 2008 Insulin signaling and the heat shock response modulate protein homeostasis in the Caenorhabditis elegans intestine during infection. J. Biol. Chem. 283: 194–201.
Muchowski, P. J., 2002 Protein misfolding, amyloid formation, and neurodegeneration: a critical role for molecular chaperones? Neuron 35: 9–12.
Mukhopadhyay, A., and H. A. Tissenbaum, 2007 Reproduction and longevity: secrets revealed by C. elegans. Trends Cell Biol. 17: 65–71.
Murphy, C. T., 2006 The search for DAF-16/FOXO transcriptional targets: approaches and discoveries. Exp. Gerontol. 41: 910–921.
Murphy, C. T., S. A. McCarroll, C. I. Bargmann, A. Fraser, R. S. Kamath *et al.*, 2003 Genes that act downstream of DAF-16 to influence the lifespan of Caenorhabditis elegans. Nature 424: 277–283.
Nedergaard, M., S. Desai, and W. Pulsinelli, 1990 Dicarboxy-dichlorofluorescein: a new fluorescent probe for measuring acidic intracellular pH. Anal. Biochem. 187: 109–114.
Oh, S. W., A. Mukhopadhyay, B. L. Dixit, T. Raha, M. R. Green *et al.*, 2006 Identification of direct DAF-16 targets controlling longevity, metabolism and diapause by chromatin immunoprecipitation. Nat. Genet. 38: 251–257.
Oka, T., R. Yamamoto, and M. Futai, 1997 Three vha genes encode proteolipids of Caenorhabditis elegans vacuolar-type ATPase. Gene structures and preferential expression in an H-shaped excretory cell and rectal cells. J. Biol. Chem. 272: 24387–24392.
Oka, T., R. Yamamoto, and M. Futai, 1998 Multiple genes for vacuolar-type ATPase proteolipids in Caenorhabditis elegans. A new gene, vha-3, has a distinct cell-specific distribution. J. Biol. Chem. 273: 22570–22576.
O'Rourke, E. J., A. A. Soukas, C. E. Carr, and G. Ruvkun, 2009 C. elegans major fats are stored in vesicles distinct from lysosome-related organelles. Cell Metab. 10: 430–435.
Peri, F., and C. Nusslein-Volhard, 2008 Live imaging of neuronal degradation by microglia reveals a role for v0-ATPase a1 in phagosomal fusion in vivo. Cell 133: 916–927.
Pilgrim, D., A. McGregor, P. Jackle, T. Johnson, and D. Hansen, 1995 The C. elegans sex-determining gene fem-2 encodes a putative protein phosphatase. Mol. Biol. Cell 6: 1159–1171.
Poon, H. F., R. A. Vaishnav, T. V. Getchell, M. L. Getchell, and D. A. Butterfield, 2006 Quantitative proteomics analysis of differential protein expression and oxidative modification of specific

proteins in the brains of old mice. Neurobiol. Aging 27: 1010–1019.
Postnikoff, S. D., M. E. Malo, B. Wong, and T. A. Harkness, 2012 The yeast forkhead transcription factors fkh1 and fkh2 regulate lifespan and stress response together with the anaphase-promoting complex. PLoS Genet. 8: e1002583.
Preston, R. A., R. F. Murphy, and E. W. Jones, 1989 Assay of vacuolar pH in yeast and identification of acidification-defective mutants. Proc. Natl. Acad. Sci. USA 86: 7027–7031.
Preston, R. A., P. S. Reinagel, and E. W. Jones, 1992 Genes required for vacuolar acidity in Saccharomyces cerevisiae. Genetics 131: 551–558.
Qiao, L., S. Hamamichi, K. A. Caldwell, G. A. Caldwell, T. A. Yacoubian *et al.*, 2008 Lysosomal enzyme cathepsin D protects against alpha-synuclein aggregation and toxicity. Mol. Brain 1: 17.
Reinke, V., H. E. Smith, J. Nance, J. Wang, C. Van Doren *et al.*, 2000 A global profile of germline gene expression in C. elegans. Mol. Cell 6: 605–616.
Rose, L. S., and K. J. Kemphues, 1998 Early patterning of the C. elegans embryo. Annu. Rev. Genet. 32: 521–545.
Rottiers, V., D. L. Motola, B. Gerisch, C. L. Cummins, K. Nishiwaki *et al.*, 2006 Hormonal control of C. elegans dauer formation and life span by a Rieske-like oxygenase. Dev. Cell 10: 473–482.
Rubinsztein, D. C., 2006 The roles of intracellular protein-degradation pathways in neurodegeneration. Nature 443: 780–786.
Sankaranarayanan, S., D. De Angelis, J. E. Rothman, and T. A. Ryan, 2000 The use of pHluorins for optical measurements of presynaptic activity. Biophys. J. 79: 2199–2208.
Shai, N., N. Shemesh, and A. Ben-Zvi, 2014 Remodeling of proteostasis upon transition to adulthood is linked to reproduction onset. Curr. Genomics 15: 122–129.
Shen, Y., J. Wollam, D. Magner, O. Karalay, and A. Antebi, 2012 A steroid receptor-microRNA switch regulates life span in response to signals from the gonad. Science 338: 1472–1476.
Shi, C., and C. T. Murphy, 2014 Mating induces shrinking and death in Caenorhabditis mothers. Science 343: 536–540.
Soukas, A. A., C. E. Carr, and G. Ruvkun, 2013 Genetic regulation of Caenorhabditis elegans lysosome related organelle function. PLoS Genet. 9: e1003908.
Stephan, J., J. Franke, and A. E. Ehrenhofer-Murray, 2013 Chemical genetic screen in fission yeast reveals roles for vacuolar acidification, mitochondrial fission, and cellular GMP levels in lifespan extension. Aging Cell 12: 574–583.
Tanida, I., T. Ueno, and Y. Uchiyama, 2014 A super-ecliptic, pHluorin-mKate2, tandem fluorescent protein-tagged human LC3 for the monitoring of mammalian autophagy. PLoS One 9: e110600.
Tepper, R. G., J. Ashraf, R. Kaletsky, G. Kleemann, C. T. Murphy *et al.*, 2013 PQM-1 complements DAF-16 as a key transcriptional regulator of DAF-2-mediated development and longevity. Cell 154: 676–690.
Tissenbaum, H. A., 2012 Genetics, life span, health span, and the aging process in Caenorhabditis elegans. J. Gerontol. A Biol. Sci. Med. Sci. 67: 503–510.
Varkey, J. P., P. J. Muhlrad, A. N. Minniti, B. Do, and S. Ward, 1995 The Caenorhabditis elegans spe-26 gene is necessary to form spermatids and encodes a protein similar to the actin-associated proteins kelch and scruin. Genes Dev. 9: 1074–1086.
Vibet, S., C. Goupille, P. Bougnoux, J. P. Steghens, J. Gore *et al.*, 2008 Sensitization by docosahexaenoic acid (DHA) of breast cancer cells to anthracyclines through loss of glutathione peroxidase (GPx1) response. Free Radic. Biol. Med. 44: 1483–1491.
Vidarsson, H., R. Westergren, M. Heglind, S. R. Blomqvist, S. Breton *et al.*, 2009 The forkhead transcription factor Foxi1 is a master regulator of vacuolar H-ATPase proton pump subunits in the inner ear, kidney and epididymis. PLoS One 4: e4471.
Vila, M., J. Bove, B. Dehay, N. Rodriguez-Muela, and P. Boya, 2011 Lysosomal membrane permeabilization in Parkinson disease. Autophagy 7: 98–100.
Vilchez, D., I. Morantte, Z. Liu, P. M. Douglas, C. Merkwirth *et al.*, 2012 RPN-6 determines C. elegans longevity under proteotoxic stress conditions. Nature 489: 263–268.
Wolf, M., F. Nunes, A. Henkel, A. Heinick, and R. J. Paul, 2008 The MAP kinase JNK-1 of Caenorhabditis elegans: location, activation, and influences over temperature-dependent insulin-like signaling, stress responses, and fitness. J. Cell. Physiol. 214: 721–729.
Yamawaki, T. M., J. R. Berman, M. Suchanek-Kavipurapu, M. McCormick, M. M. Gaglia *et al.*, 2010 The somatic reproductive tissues of C. elegans promote longevity through steroid hormone signaling. PLoS Biol. 8: e1000468.
Yin, D., 1996 Biochemical basis of lipofuscin, ceroid, and age pigment-like fluorophores. Free Radic. Biol. Med. 21: 871–888.

Communicating editor: M. P. Colaiacovo